Neuroprotective Potential of Laurus nobilis Antioxidant Polyphenol-Enriched Leaf Extracts

ARTICLE *in* CHEMICAL RESEARCH IN TOXICOLOGY · FEBRUARY 2014

Impact Factor: 3.53 · DOI: 10.1021/tx5000415 · Source: PubMed

Chemical Research in Toxicology

Article

pubs.acs.org/crt

Neuroprotective Potential of *Laurus nobilis* Antioxidant Polyphenol-Enriched Leaf Extracts

Severina Pacifico,*[,†] Marialuisa Gallicchio,[†] Peter Lorenz,[‡] Sarina M. Duckstein,[‡] Nicoletta Potenza,[†] Silvia Galasso,[†] Sabina Marciano,[†] Antonio Fiorentino,[†] Florian C. Stintzing,[‡] and Pietro Monaco[†]

[†]Department of Environmental Biological and Pharmaceutical Sciences and Technologies, Second University of Naples, Via Vivaldi 43, I-81100 Caserta Italy

[‡]WALA Heilmittel GmbH, Dorfstraße 1, 73087 Bad Boll/Eckwälden, Germany

ABSTRACT: Oxidative stress has been proposed to be an important factor in the pathogenesis of Alzheimer's disease (AD), playing a central role in amyloid β-protein (Aβ) generation and neuronal apoptosis. Oxidative damage directly correlates with the presence of Aβ deposits. Aβ and oxidative stress jointly induce neuronal death, Aβ deposits, gliosis, and memory impairment in AD. In order to counteract AD neurodegeneration, the inhibition of the vicious cycle of Aβ generation and oxidation is an attractive therapeutic strategy, and antiamyloidogenic and antioxidant herbal drugs could represent an alternative and valid approach. In this context, an alcoholic extract from *Laurus nobilis* leaves (LnM) and seven fractions obtained therefrom were of interest. All extracts prepared through extractive and chromatographic techniques were phytochemically studied by chromatographic techniques including gas chromatography–mass spectrometry (GC-MS) and liquid chromatography–tandem mass spectrometry (LC-MS^n). The potential antioxidant efficacy of the obtained fractions was screened by DPPH$^\bullet$ and ABTS$^{\bullet+}$ assays, as well as specific assay media characterized from the presence of highly reactive ROS and RNS species (ROO$^\bullet$, OH$^\bullet$, $O_2^{\bullet-}$, and NO). In order to evaluate the preparation of safe and nontoxic extracts, MTT, SRB, and LDH assays toward SH-5YSY and SK-N-BE(2)-C human neuronal cell lines, as well as on C6 mouse glial cell line, were performed. The apoptosis-inducing properties by spectroscopic evaluation of the extracts' ability to activate caspase-3 and by a DNA fragmentation assay were also investigated. Data thus obtained allowed us to state the absence of toxic effects induced by phenolic-rich fractions (LnM, LnM-1, LnM-1a, LnM-1b, and LnM-2c), which at the same time exerted significant cytoprotective and antioxidant responses in hydrogen peroxide and Aβ(25–35)-fragment-oxidized cell systems. The potential antiamyloidogenic efficacy of *Laurus nobilis* leaf polar extracts in the Aβ(25–35) fragment oxidized cell systems was further analyzed by Congo red staining.

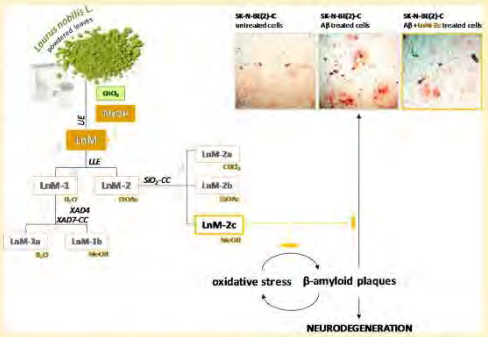

1. INTRODUCTION

Alzheimer's disease (AD) is an aging-related progressive neurodegenerative disease characterized by massive neuronal and synaptic loss and accompanied by neuropathological changes, such as neurofibrillary tangles and senile plaques in the hippocampus, neocortex, and subcortical structures.[1] The amyloid plaques consist of different forms of the amyloid β (Aβ) derivatives of the amyloid precursor protein (APP), which are produced by an incorrect cleavage of APP by two proteolytic enzymes, β- and γ-secretases.[2]

One of the most well-known and studied effects of Aβ is its capacity to induce but also being itself induced by oxidative stress.[3] This is caused by reactive nitrogen and/or oxygen species as an imbalance between the formation of cellular oxidants and antioxidative processes.[4] The central nervous system appears to be particularly vulnerable to oxidative stress because of the brain's high oxygen consumption rate, its high lipid content, the presence of transition metals such as iron, and because of its deficient antioxidative defense mechanisms.[5−7] Oxidative stress activates microglia and astrocytes inducing the expression of immuno-active molecules, secretion of cytotoxic factors, and secretion of pro-inflammatory signaling molecules altogether contributing to Aβ generation and accumulation. Aβ-induced oxidative stress leads to apoptotic neuronal cell death that can be inhibited by antioxidants.[8]

Recent *in vitro* and *in vivo* studies recognized naturally occurring phytochemicals, such as isolated resveratrol or curcumin, but also plant extracts enriched in phenolic antioxidants as alternative therapeutic agents for the prevention and treatment of AD. *Ginkgo biloba* extracts showed significant neuroprotective effects in murine models and improved cognitive function in AD patients through their ability to act as free radical scavengers and/or counteract Aβ-induced free radical production. It was also suggested that *Ginkgo biloba* preparations were able to regulate the APP processing by the α-secretase pathway activation.[9] Aqueous garlic extracts showed

Received: December 4, 2013
Published: February 18, 2014

antiamyloidogenic properties inhibiting Aβ fibril formation and also defibrillating Aβ preformed fibrils.[10]

Moderate consumption of red wine reduced the incidence of AD dementia and can benefit the disease course. Both grape berries and red wine derived therefrom are rich in antioxidants with neuroprotective properties. In particular, it was observed that the treatment of murine models of AD with Cabernet Sauvignon red wine[11] reduced the neuropathology and cognitive deterioration promoting the proteolytic cleavage of nonamyloidogenic APP protein and thereby inhibiting Aβ genesis. Oral administration of a polyphenolic extract from grape seeds in murine models was able to inhibit the formation of fibrillar aggregates and was accompanied by the accumulation of antioxidants such as catechin and its isomer epicatechin both in the bloodstream and in the brain tissue.[12] This scientific and epidemiological evidence, emphasizing the key role of phyto-antioxidants in the prevention of Alzheimer's disease and other dementias, lays the foundation to the present work whose objective was the evaluation of neuroprotective and antioxidant analysis of *Laurus nobilis* L. leaf extracts.

The laurel, abundant in the Mediterranean basin, was already the object of a previous investigation,[13] in which a leaf chloroform extract and its derived apolar fractions exhibited neuroprotective action toward three nervous system cell lines, which allowed us to state their potential role in brain cancer therapy. In order to complement the knowledge on laurel neuroprotective properties, present work addresses the alcoholic extract, obtained from $CHCl_3$-pre-extracted and dried leaf powder.

2. MATERIALS AND METHODS

2.1. Reagents and Chemicals. All of the solvents and reagents used for assessing antioxidant screening were purchased from Sigma-Aldrich (Buchs, Switzerland) except for ABTS [2,2′-azinobis-(3-ethylbenzothiazolin-6-sulfonic acid)], which was from Roche Diagnostics (Roche Diagnostics, Mannheim, Germany). Cell culture media and reagents for cytotoxicity testing were purchased from Invitrogen (Paisley, UK), and MTT [3-(4,5-dimethyl-2-thiazolyl)-2,5-diphenyl-2*H*-tetrazolium bromide], SRB (sulforhodamine B), INT [(2-(4-iodophenyl)-3-(4-nitrophenyl)-5-phenyl-2*H*-tetrazolium chloride)], Aβ(25−35) fragment, phenazine methosulfate, and lactic acid were from Sigma-Aldrich Chemie. For chromatographic purposes, acetonitrile (LC-MS grade) and formic acid (98%, for mass spectrometry), both purchased from Sigma-Aldrich (Buchs, Switzerland), as well as purified water from a Purelab Option-Q system (Elga Berkefeld GmbH, Celle, Germany), were used.

2.2. Plant Collection and Fractionation. Leaves from *Laurus nobilis* were collected in Caserta (Italy) in May 2011 and identified by Dr. Assunta Esposito of the Second University of Naples. A voucher specimen (voucher number: CE000215) has been deposited at the Herbarium of the Department of Environmental, Biological and Pharmaceutical Sciences and Technologies of the Second University of Naples. After drying in a thermo-ventilated oven at 40 °C for 7 days, leaves (25.0 g) were powdered in a mill and extracted by sonication (Dr. Hielscher UP 200S, Germany) for 1 h, using $CHCl_3$ as extracting solvent. Then the samples were centrifuged at 2,044*g* for 10 min in a Beckman GS-15R centrifuge (Beckman Coulter, Milano, Italy) fitted with rotor S4180. The plant material (Figure 1) underwent four sonication cycles (each sonication cycle was 60 min) using MeOH as extracting solvent (75.0 mL for each sonication cycle). The supernatant was dried under vacuum by a rotary evaporator (Heidolph Hei-VAP Advantage, Germany) to yield a crude extract (6.0 g, LnM), which was afterward fractionated through discontinuous liquid−liquid extraction (H_2O/EtOAc). Thus, an aqueous (LnM-1) and an organic fraction (LnM-2) were obtained. The first one (4.1 g), further chromatographed using XAD-4 (200.0 g) and XAD-7 (200.0 g) resins,

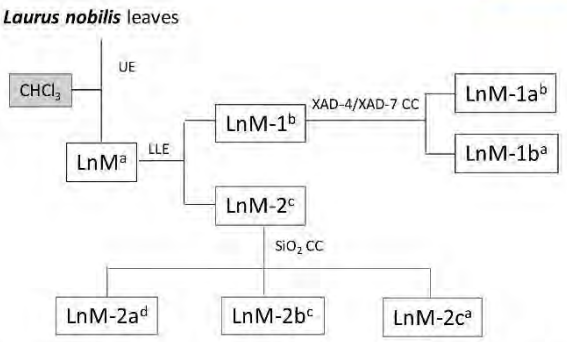

Figure 1. Fractionation scheme of LnM extract from *Laurus nobilis* leaves. a, MeOH; b, H_2O; c, EtOAc; d, $CHCl_3$. UE = ultrasound extraction; LLE = liquid liquid extraction; CC = column chromatograpy.

and H_2O (500.0 mL) and MeOH (300.0 mL) as eluting solvents, allowed us to obtain LnM-1a (1.0 g) and LnM-1b (1.6 g) fractions. The organic fraction (1.1 g) was chromatographed on silica gel (11.0 g) using $CHCl_3$ (150.0 mL), EtOAc (150.0 mL), and MeOH (150.0 mL) as eluents. Three fractions were thus obtained: LnM-2a (236.0 mg), LnM-2b (477.0 mg), and LnM-2c (196.0 mg).

2.3. RP-HPLC-ESI-MS/MS Analyses. Chromatographic analyses were carried out on an Agilent 1200 HPLC system (Agilent Technologies Inc., Palo Alto, USA), equipped with a binary pump, a vacuum degasser, an autosampler, a thermostatic column compartment, and a diode array detector. A SunFire C18-reversed phase column (5 μm particle size, 150 × 2.1 mm i.d., Waters Corporation, Milford, MA USA) was used for chromatographic separation at 25 °C and a flow rate of 0.21 mL/min. The UV detection of phenolic derivatives (Figure 2) was performed at 280 and 300 nm. The mobile phase consisted of 0.2% formic acid in water (v/v; mobile phase A) and acetonitrile (mobile phase B). Starting with 0% B for 5 min, a linear gradient was followed to 33% B at 105 min, then increasing to 100% B at 110 min, continuing for 5 min, before re-equilibration to starting conditions. The samples (30.0 mg each) were dissolved in an MeOH/water mixture (1/4; v/v), sonicated for 2 min, and filled in a volumetric flask on a final volume of 25.0 mL. Then, the samples were centrifuged at 19,064*g* (5 min) before use. The injection volume of each sample was 30.0 μL. The LC system was coupled to an HCTultra ion trap (Bruker Daltonik GmbH, Bremen, Germany) with an ESI ion source operating in the negative mode with the following parameters: HV voltage, 4000 V; dry gas flow (N_2), 9.00 L/min with a capillary temperature set at 365 °C; and nebulizer pressure, 35 psi. Mass spectra were recorded between m/z 50−2000 with a compound stability and trap drive level of 100%. To obtain further structural information, these ions were trapped and fragmented to yield the precursor product patterns of the analytes. MS^n data were acquired in the auto MS/MS mode. Instrument control and data processing software used were Agilent ChemStation B.01.03 (Agilent Technologies Inc., Palo Alto, USA) as well as EsquireControl and DataAnalysis V6.1 (Bruker Daltonik GmbH, Bremen, Germany). The constituents were identified by comparison of their specific chromatographic data including UV spectra and MS/MS fragmentation patterns with literature data and reference compounds.

2.4. Scavenging Capacity Assessment. Because multiple reaction characteristics and mechanisms as well as different phase localizations are usually involved, no single assay can accurately reflect all types of radical sources or antioxidants in a mixed or complex system.[14] Thus, six different *in vitro* antiradical assays were employed.[15−17] MeOH extract and the fractions derived therefrom, previously dissolved in DMSO as stock solutions of 125.0 mg/mL, were evaluated at different concentration levels (DMSO final concentration was equal to 0.1% (v/v)). Tests were carried out performing three replicate measurements for three samples (n = 3) of each extract (in total, 3 × 3 measurements). Recorded activities were

dx.doi.org/10.1021/tx5000415 | *Chem. Res. Toxicol.* 2014, 27, 611−626

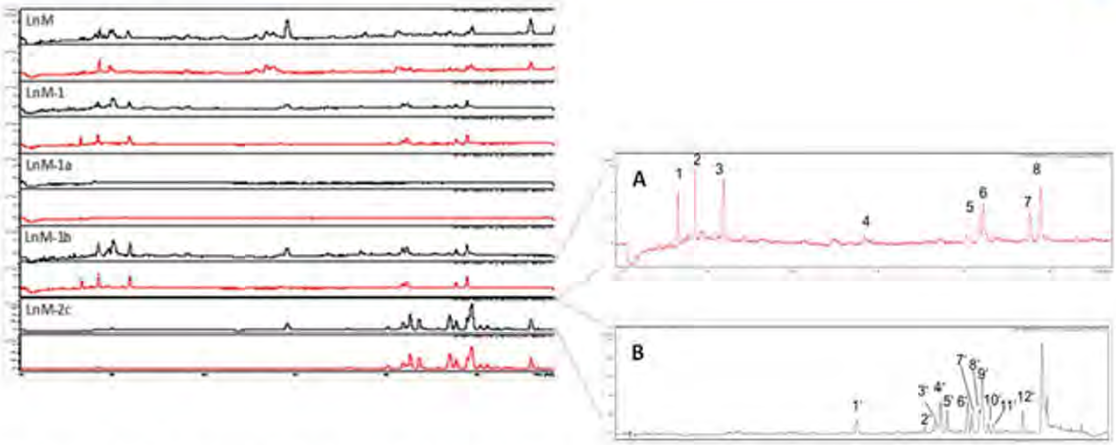

Figure 2. RP-HPLC-DAD chromatograms of MeOH extracts (LnM) and polar fractions therefrom. (A) LnM-1b HPLC-DAD Chromatogram at 280 nm; (B) LnM-2c HPLC-DAD Chromatogram at 300 nm.

compared to a blank. Results are the mean ± SD values. Student's *t*-test was applied in order to determine statistical significance (significance level was set at $P < 0.05$).

2.4.1. Determination of DPPH• Scavenging Capacity. In order to estimate the DPPH• (2,2-diphenyl-1-picrylhydrazyl) scavenging capability, investigated extracts (2.5, 5.0, 10.0, 25.0, 50.0, and 100.0 μg/mL, final concentration levels) were dissolved in a DPPH• methanol solution (9.4×10^{-5} M; 1.0 mL) at room temperature. After 10 min, when the reaction has gone to completion, the absorption at 515 nm was measured by a Shimadzu UV-1700 spectrophotometer in reference to a blank. The results were expressed in terms of the percentage decrease of the initial DPPH• radical absorption by the test samples.

2.4.2. Determination of $ABTS^{\bullet+}$ Scavenging Capacity. The determination of $ABTS^{\bullet+}$ solution scavenging capacity was estimated as previously reported. The ABTS radical cation was generated by reacting ABTS ([2,2′-azinobis-(3-ethylbenzothiazolin-6-sulfonic acid)]; 7.0 mM) and potassium persulfate (2.45 mM). The mixture was allowed to stand in the dark at room temperature for 12−16 h. Thus, the $ABTS^{\bullet+}$ solution was diluted with PBS (pH 7.4) in order to reach an absorbance of 0.70 at 734 nm. *L. nobilis* extracts (2.5, 5.0, 10.0, 25.0, 50.0, and 100.0 μg/mL, final concentration levels) were dissolved in 1.0 mL of diluted $ABTS^{\bullet+}$ solution. After 6 min of incubation, the absorption at 734 nm was measured by a Shimadzu UV-1700 spectrophotometer in reference to a blank. The results were expressed in terms of the percentage decrease of the initial $ABTS^{\bullet+}$ absorption by the test samples.

2.4.3. Determination of Oxygen Radical Absorbance Capacity (ORAC). The ORAC assay was performed as follows: each extract (20 μL; 1.0, 2.5, and 5.0 μg/mL, final concentration levels) and fluorescein (120.0 μL; 70 nM, final concentration) were preincubated for 15 min at 37 °C in 75 mM phosphate buffer (pH 7.4). Then, 2,2′-azobis-(2-amidinopropane)-dihydrochloride (AAPH) solution (60.0 μL; 12 mM, final concentration) was rapidly added. In parallel with the test samples, a blank (FL + AAPH) and solutions of the reference antioxidant Trolox (1−8 μM, final concentration levels) were properly prepared in PBS. The fluorescence decay (λ_{ex} = 485 nm, λ_{em} = 525 nm) was recorded every minute for 120 min using a Tecan SpectraFluor fluorescence and absorbance reader. Antioxidant curves (fluorescence vs time) were normalized to the curve of the blank. From the normalized curves, the area under the fluorescence decay curve (AUC) was calculated. Linear regression equations between net AUC ($AUC_{antioxidant} - AUC_{blank}$) and antioxidant concentration were calculated for all of the samples. The antioxidant activity (ORAC value) was calculated by using the Trolox calibration curve. The ORAC values were expressed as Trolox equivalents (μM).

2.4.4. Determination of $O_2^{\bullet-}$ Scavenging Capacity. The inhibition of nitroblue tetrazolium (NBT) reduction by photochemically generated $O_2^{\bullet-}$ was used to determine the superoxide anion radical scavenging activity of the extracts according to the literature. *L. nobilis* extracts (2.5, 5.0, 10.0, 25.0, 50.0, and 100.0 μg/mL, final concentration levels) were dissolved at room temperature in 3.0 mL of a reaction mixture containing sodium phosphate buffer (50.0 mM, pH 7.8), methionine (13.0 mM), riboflavin (2.0 μM), EDTA (100.0 μM), and NBT (75.0 μM). The $O_2^{\bullet-}$ production was followed by monitoring the increase in absorbance at 560 nm after 10 min of illumination with a fluorescent lamp.

2.4.5. Determination of OH• Scavenging Capacity. Fe(III)-EDTA-H_2O_2 solutions were used as the hydroxyl radical (OH•) generating system (Fenton reaction), and the radical scavenging capabilities of *L. nobilis* extracts (2.5, 5.0, 10.0, 25.0, 50.0, and 100.0 μg/mL, final concentration levels) were evaluated by the determination of malondialdehyde (MDA) from the oxidative degradation of 2-deoxyribose. The reagent mixture, consisting of aqueous H_2O_2 (100.0 μM), EDTA (100.0 μM), $FeCl_3$ (100.0 μM), and ascorbic acid (100.0 μM) in KH_2PO_4/KOH buffer (10 mM, pH 7.4), was incubated at 37 °C for 1 h. Then, 2-deoxyribose (28 mM) was added. The reaction mixture was allowed to stand at 37 °C for 5 min. Thus, 1.0 mL of the diluted reagent mixture was added into tubes containing test samples, which were incubated at 37 °C for 1 h. To each tube, 1.0 mL of a 1% TBA (thiobarbituric acid) solution in 50 mM NaOH and 1.0 mL of a solution at 2.8% of TCA (trichloroacetic acid) was added and placed in a water bath at 90 °C for 30 min before taking the reading at 532 nm.

2.4.6. Determination of NO Scavenging Capacity. Nitric oxide (NO) generated from sodium nitroprusside (SNP) was measured by the Griess reagent. *L. nobilis* extracts (25.0 μL; 2.5, 5.0, 10.0, 25.0, 50.0, and 100.0 μg/mL, final concentration levels) were added to SNP (1.0 mL, 15 mM) in 0.2 M NaH_2PO_4/Na_2HPO_4 buffer, pH 7.4. The reaction mixtures were incubated at 37 °C for 180 min. Then, 80.0 μL was transferred into a 96-multiwell plate and mixed with 50.0 μL of Griess reagent solution A (1% sulfanilamide w/v in 10% HCl 37% v/v). After 5 min, 50.0 μL of Griess reagent solution B (0.1% *N*-(1-naphthyl)ethylenediaminedihydrochloride) was added. After 10 min of incubation at room temperature, the absorbance was measured at 540 nm, using a Tecan SpectraFluor reader, and referred to the absorbance of $NaNO_2$ standard solutions, treated in the same way with the Griess reagents, by means of a calibration curve.

2.5. Cytotoxicity Assessment. Cytotoxicity assays which use different parameters associated with cell death and proliferation were performed.[13] Samples of each extract were prepared as stock solutions of 125.0 mg/mL in DMSO. They were further diluted in cell culture medium to appropriate final dose levels (DMSO final concentration

was equal to 0.1% (v/v)). Tests were carried out performing 12 replicate (n = 12) measurements for three samples of each extract (in total, 12 × 3 measurements). Recorded activities were compared to an untreated blank arranged in parallel to the samples. Results are the mean ± SD values. Student's t-test was applied in order to verify statistical significance (significance level was set at $P < 0.05$).

2.5.1. Cell Cultures. The rat C6 glioma cell line and human SH-SY5Y neuroblastoma cells were purchased from ATCC (American Type Culture Collection); SK-N-BE(2)-C human bone marrow neuroblastoma cells were purchased from ICLC (Interlab Cell Line Collection) at Istituto Nazionale per la Ricerca sul Cancro, Genoa (Italy). Rat C6 and SH-SY5Y cell lines were grown in DMEM high glucose medium supplemented with 10% fetal bovine serum, 50.0 U/mL penicillin, and 100.0 μg/mL streptomycin, at 37 °C in a humidified atmosphere containing 5% CO_2. The SK-N-BE(2)-C cell line was plated and grown under the same conditions, except that RPMI 1640 was used instead of DMEM.

2.5.2. MTT Cell Viability Test. The MTT test allows the assessment of cell viability by determining the levels of activity of mitochondrial dehydrogenases able to transform 3-(4,5-dimethyl-2-thiazolyl)-2,5-diphenyl-2*H*-tetrazolium (MTT) into a colored formazan product.

C6, SH-SY5Y, and SK-N-BE(2)-C cell lines were seeded in 96-multiwell plates at a density of 1.0 × 10^4 cells/well. After 24 h of incubation, cells were treated with extracts from *L. nobilis* at six dose levels (2.5, 10.0, 25.0, 50.0, 100.0, and 250.0 μg/mL). At 24, 48, and 72 h of incubation, cells were treated with 150.0 μL of MTT (0.50 mg/mL) and dissolved in the culture medium for 1 h at 37 °C in a 5% CO_2 humidified atmosphere. The MTT solution was then removed, and 100.0 μL of DMSO was added to dissolve the produced formazan dye. Finally, the absorbance at 570 nm of each well was determined using a Tecan SpectraFluor fluorescence and absorbance reader. Cell viability was expressed as the percentage of mitochondrial redox activity of the cells treated with the extracts compared to the untreated control. Cell viability inhibition (CVI, %) was calculated using the following formula:

$$[(\mathrm{Abs}_{\text{untreated cells}}) - (\mathrm{Abs}_{\text{treated cells}})/(\mathrm{Abs}_{\text{untreated cells}})] \times 100$$

The dose of each extract able to inhibit cell viability by 50% (ID_{50} value, μg/mL) was determined.

2.5.3. SRB Cell Viability Test. The sulforhodamine B (SRB) assay is used for cell density determination, based on the measurement of the cellular protein content.[18] C6, SH-SY5Y, and SK-N-BE(2)-C cell lines were seeded in 96-multiwell plates at a density of 1.0 × 10^4 cells/well. After 24 h of incubation, cells were treated with extracts from *L. nobilis* at six dose levels (2.5, 10.0, 25.0, 50.0, 100.0, and 250.0 μg/mL). At 24, 48, and 72 h of incubation, cells were fixed with ice-cold TCA (10% w/v, 40 μL) for 1 h at 4 °C. The plates were washed five times in distilled water and allowed to dry. Then, 50 μL of sulforhodamine B (SBR, 0.4% w/v in 1% aqueous *acetic acid*) solution was added to each well of the dried 96-well plates and incubated at room temperature for 30 min. In order to remove unbound dye, the plates were quickly washed with 1% aqueous acetic acid and dried subsequently. The bound SRB was solubilized by adding 100 μL of 10 mM unbuffered Tris base (pH 10.5) to each well and shaking for 5 min on a shaker platform. Finally, the absorbance at 570 nm of each well was measured using a Tecan SpectraFluor fluorescence and absorbance reader. Cell viability inhibition (CVI, %) was calculated using the following formula:

$$[(\mathrm{Abs}_{\text{untreated cells}}) - (\mathrm{Abs}_{\text{treated cells}})/(\mathrm{Abs}_{\text{untreated cells}})] \times 100$$

The dose of each extract able to inhibit cell viability by 50% (ID_{50} value, μg/mL) was determined.

2.5.4. Lactate Dehydrogenase (LDH) Leakage Assay. The lactate dehydrogenase (LDH) leakage assay is a colorimetric assay for the quantification of cell death and cell lysis based on the measurement of LDH released from the cytosol of damaged cells into the supernatant. LDH activity can be determined by a coupled enzymatic reaction: LDH oxidizes lactate to pyruvate, which then reacts with tetrazolium salt 2-(4-iodophenyl)-3-(4-nitrophenyl)-5-phenyltetrazolium chloride (INT) to form a water-soluble formazan dye. The increase in the amount of formazan produced in culture supernatant directly correlates to the increase in the number of lysed cells.

C6, SH-SY5Y, and SK-N-BE(2)-C cell lines were seeded in 24-multiwell plates at a density of 4.0 × 10^4 cells/well. Twenty-four hours after seeding, the cells were treated with extracts (100.0 μg/mL) from *L. nobilis*. The exposure times were 24 h, 48 h, and 72h. Then, each supernatant (100.0 μL) was treated with 100.0 μL of the reaction mixture (0.7 mM INT; 54.0 mM lactic acid; 0.3 mM phenazine methosulfate; and 0.8 mM NAD^+ in 0.2 M Tris-HCl pH 8.0) in a 96-well plate. The reaction was carried out for 45 min in the dark under gentle stirring at 37 °C and stopped by the addition of 1.0 M HCl (50.0 μL). The absorbance was read at 492 nm by a Tecan SpectraFluor fluorescence and absorbance reader. Data obtained were expressed in reference to a blank prepared using a Triton X-100 (1.0%) solution. The amount of enzyme activity detected in the culture supernatant reflects the membrane integrity and correlates with the proportion of lysed cells. Hence, cell vitality is inversely proportional to the LDH released. LDH release percentage was calculated using the following formula:

$$[(\mathrm{Abs}_{\text{treated cells}} - \mathrm{Abs}_{\text{untreated cells}})/(\mathrm{Abs}_{\text{Triton-X100treated cells}} - \mathrm{Abs}_{\text{untreated cells}})] \times 100$$

2.6. Assessment of Apoptosis-Inducing Activities. *2.6.1. Caspase-3 Activation Assay.* Caspases are crucial mediators of programmed cell death. Among them, caspase-3 (also known as CPP32, Yama or apopain) is a frequently activated death protease, catalyzing the specific cleavage of many key cellular proteins. Caspase-3 activation was detected through the Caspase-3/CPP32 Colorimetric Kit (Invitrogen), following the protocol described by the manufacturer. The Caspase-3 colorimetric protease assay provides a simple and convenient means for the quantification of caspases that recognize the amino acid sequence, DEVD. The substrate, DEVD-*p*NA, is composed of the chromophore, *p*-nitroanilide (*p*NA), and a synthetic tetrapeptide, DEVD (Asp-Glu-Val-Asp), which is the upstream amino acid sequence of the caspase-3 cleavage site in PARP (Poly ADP ribose polymerase). Upon cleavage of the substrate by caspase-3, free *p*NA light absorbance can be spectrophotometrically quantified. Comparison of the absorbance of *p*NA from an apoptotic sample with a control allows for the determination of the fold increase in caspase-3 activity. Briefly, cells were plated in 6-multiwell plates at a density of 1.6 × 10^5 cells/well. Twenty-four hours after seeding, the cells were treated with extracts (100.0 μg/mL) from *L. nobilis* and incubated for another 48 h. Cells were resuspended in 50.0 μL of chilled cell lysis buffer and incubated on ice for 10 min. After centrifugation at 10,000*g* and 4 °C for 1 min, the supernatant (cytosol extract) was transferred to a fresh tube and put on ice. Protein in the supernatant was quantified by the Lowry method with bovine serum albumin as standard. Each cytosol extract was diluted to a concentration of 100.0 μg of protein per 50.0 μL of cell lysis buffer (2 mg/mL). Thus, 50.0 μL of 2× reaction buffer (containing 10.0 mM dithiothreitol) and 5.0 μL of the 4 mM DEVD-*p*NA caspase 3 substrate (200.0 μM final concentration of each) were added. After 2 h of incubation at 37 °C, the formation of *p*-nitroanilide was measured at 405 nm by the use of a Tecan SpectraFluor fluorescence and absorbance reader.

Caspase-3 activation percentage was calculated using the following formula:

$$[(\mathrm{Abs}_{\text{treated cells}} - \mathrm{Abs}_{\text{blank}})/\mathrm{Abs}_{\text{blank}}] \times 100$$

2.6.2. DNA Fragmentation Assay. Oligonucleosomal fragmentation of genomic DNA is one of the hallmarks of apoptosis. It can be detected as a ladder pattern on agarose gel electrophoresis. Cells were seeded in 6-multiwell plates at a density of 1.6 × 10^5 cells/well. Twenty-four hours after seeding, the cells were treated with extracts (100.0 μg/mL) from *L. nobilis* and incubated for another 48 h. In parallel, an untreated control was set up. Cells were washed with PBS, harvested by centrifugation (6000 rpm, 5 min), and lysed by incubating at 55 °C for 2 h in lysis buffer (50 mM Tris-HCl pH 8.0, 10.0 mM EDTA, and 0.5% SDS) with proteinase K (0.5 mg/mL).

dx.doi.org/10.1021/tx5000415 | *Chem. Res. Toxicol.* 2014, 27, 611–626

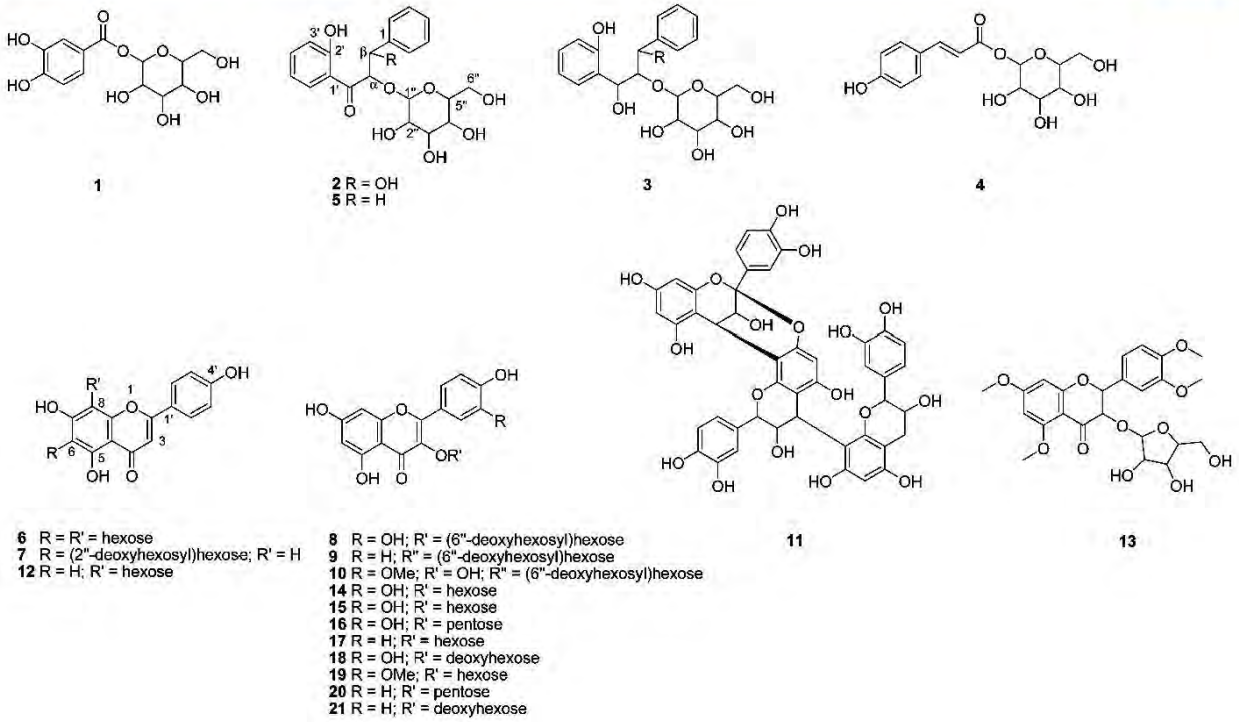

Figure 3. Main metabolites identified from polar fractions of the LnM extract.

Then, genomic DNA was isolated by ethanol precipitation. In brief, DNA solution was mixed with 2.5 volumes of cold absolute ethanol, in the presence of sodium acetate (0.1 volumes, 3M, pH 5.2), and incubated at −80 °C; DNA was pelletted by centrifugation (13000 rpm, 15 min), washed by 70% ethanol. Dried pellets were dissolved in distilled water and incubated at 37 °C for 30 min with Rnase A to a final concentration of 100 μg/mL. DNA samples were quantified using NanoDrop 2000/2000c Spectrophotometers (ThermoScientific, Wilmington, DE, USA) and stored at 4 °C. Each DNA sample (3.0 μg) was loaded onto 2.0% agarose gel (containing 10 μg/mL ethidium bromide) in 1× TAE buffer, along with a molecular weight marker (100 bp ladder, Amersham Pharmacia).

2.7. Cytoprotection Screening. *2.7.1. Determination of Cytoprotective Effects in H_2O_2 Induced Oxidation Cell Systems.* SK-N-BE(2)-C, and SH-5YSY cell lines were seeded in 96-multiwell plates at a density of 1.0×10^4 cells/well. After 24 h of incubation, cells were cotreated with *Laurus nobilis* leaf extracts (25.0, 50.0, and 100.0 μg/mL, final concentration levels) and H_2O_2 (400.0 μM) for 24 h. After the treatment period, cell viability inhibition was assessed by the MTT assay.

2.7.2. Determination of the Cytoprotective Effect in Aβ(25−35) Induced Oxidation Cell Systems. As it is known that exposure of neuronal cell lines to the β-amyloid peptide causes an increase of neuronal damage mediated by the induction of ROS synthesis and to evaluate the antioxidant effectiveness of investigated extracts against β-amyloid induced neurotoxicity, the Aβ(25−35) fragment was used. The Aβ(25−35) fragment was dissolved in DMSO (12.5 mM, final concentration) and stored at −20 °C until use. SK-N-BE(2)-C and SH-5YSY cell lines were seeded in 96-multiwell plates at a density of 1.0×10^4 cells/well. After 24 h of incubation, cells were treated with *Laurus nobilis* leaf extracts (25.0, 50.0, and 100.0 μg/mL) and neurotoxic Aβ(25−35) peptide (100.0 μM) for 24 h. After the treatment period, cell viability inhibition was assessed by the MTT assay.

2.8. Measurement of Intracellular ROS Formation. The levels of intracellular reactive oxygen species (ROS) were determined by the change in fluorescence resulting from the oxidation of the fluorescent probe 2′,7′-dichlorofluorescein diacetate (DCFH-DA). When applied to intact cells, DCFH-DA readily diffuses through the cell membrane and is hydrolyzed enzymatically by intracellular esterases to non-fluorescent DCFH. In the presence of ROS, DCFH is oxidized to highly fluorescent DCF, whose fluorescent intensity is proportional to the amount of ROS formed intracellularly.[19]

The SK-N-BE(2)-C cell line, seeded in 96-multiwell plates at a density of 1.0×10^4 cells/well, was incubated with DCFH-DA (10 μM) in PBS for 30 min.[20] At the end of incubation, DCFH-DA solution was removed, and cells were cotreated with *Laurus nobilis* leaf extracts (25.0, 50.0, and 100.0 μg/mL) and H_2O_2 (400.0 μM) or Aβ(25−35) peptide (100.0 μM). Trolox (2.0, 4.0, 8.0, and 16.0 mM), a water-soluble analogue of vitamin E, was used as the positive standard. The fluorescence intensity was measured at 485 nm excitation and 535 nm wavelength in a Tecan SpectraFluor fluorescence and absorbance reader. Results are expressed as percentages relative to oxidized cell lines arbitrarily set at 100%.

2.9. Congo Red Staining Assay. Congo red (CR), an azo dye that contains naphthalenesulfonic acid groups, is the most popular dye used as a probe for diagnosing amyloidosis. Congo red binding increases the natural anisotropy of amyloid. This CR-induced (positive) anisotropy displaying a green color is the hallmark of all amyloids and is therefore used in the diagnosis of amyloidosis.[21]

The SK-N-BE(2)-C cell line was seeded in 6-multiwell plates at a density of 1.6×10^5 cells/well. After 24 h of incubation, cells were treated with LnM-2a and LnM2-c extracts (100.0 μg/mL) and neurotoxic Aβ(25−35) peptide (100.0 μM) for 24 h. After the treatment period, cells were fixed in ice-cold 100% methanol and then stained for 45 min with Congo red solution. For this purpose, Congo red powder (0.5g) was dissolved in EtOH (80.0 mL) and then mixed with 20.0 mL of an aqueous NaCl solution (10.0%, w/v). After several quick dips in water, cell dehydration was accomplished by washing sequentially in 95% ethanol and 100% ethanol. Stained cells were visualized using a Nikon Eclipse E200 light microscope.

dx.doi.org/10.1021/tx5000415 | *Chem. Res. Toxicol.* 2014, 27, 611−626

Table 1. LC-MS/MS and UV Spectral Data of Identified Compounds in LnM-1b (1−10) and LnM-2c (9−10 and 11−21) Extracts

						pseudomolecular ions [m/z] in [MS]$^-$ mode		
peak	compd	compound assignment	MW [Da]	t_R [min]	UV_{max} [nm]	MS	MS^2	MS^3
1	**1**	3,4-dihydroxybenzoic acid hexoside	316	16.8	208, 234 (sh), 315	631[a], 315[b]	153[d]	123, 109
2 coelution	**2**	2′,β -dihydroxy-α,β-dihydrochalcone-α-*O*-hexoside	420	18.8	298	419[b], 285	257[d]	221, 206
	3	1-(2′-hydroxyphenyl)-1-hydroxyphenylpropan-α-*O*-hexoside	452	19.0	298	451[c]	405[b]	243[d], 225
3 coelution	**4**	coumaric acid-hexoside	326	22.1	292	651[a], 325[b]	163[d]	119
	5	2′-hydroxy-α,β-dihydrochalcone-α-*O*-hexoside	450	22.3	292	449[c]	403[b]	241[d], 223, 179
4	**6**	apigenin-6,8-di-*C*-hexoside	594	38.5	208	593[b]	575, 503, 473[e], 383, 353[f]	383, 353
5	**7**	apigenin-6-*C*-(2″-*O*-deoxyhexosyl)-hexoside	578	51.9	270, 336	577[b]	457, 413	341, 293
6	**8**	quercetin-3-*O*-(6″-*O*-deoxyhexosyl)-hexoside	610	52.4	256, 354	609[b]	301[g]	271, 255, 179, 151
7/7′	**9**	kaempferol-3-*O*-(6″-*O*-deoxyhexosyl)-hexoside	594	57.8	264, 348	593[b]	285[g]	257, 229, 163
8/8′	**10**	(iso)rhamnetin-3-*O*-(6″-*O*-deoxyhexosyl)-hexoside	625	59.0	254, 356	623[b]	315[g], 300[h]	300, 271, 255
1′	**11**	cinnamtannin B1	864	39.5	200, 226 (sh), 280	863[b]	711, 693	693, 559, 541, 407, 289
2′	**12**	8-*C*-hexosyl apigenin	432	50.1	268, 338	431[b]	341, 311[e]	283, 117
3′	**13**	tetra-methoxy-dihydroquercetin-3-*O*-pentoside	492	51.6	270, 338	491[b]	359[i]	344, 329
4′	**14**	quercetin-3-*O*-hexoside (isomer 1)	464	52.8	256, 354	463[b]	301[d], 300[j]	271, 255, 179, 151
5′	**15**	quercetin-3-*O*-hexoside (isomer 2)	464	53.9	256, 354	463[b]	301[h]	271, 179, 151
6′ coelution	**16**	quercetin-3-*O*-pentoside	434	56.8	264, 348	867[a], 433[b]	301[i], 300[k]	271, 255, 179, 151
	17	kaempferol-3-*O*-hexoside	448	57.3	264, 348	895[a], 447[b]	285[d], 284[j]	255, 227
9′	**18**	quercetin-3-*O*-deoxyhexoside	448	59.4	256, 348	895[a]; 447[b]	301[h]	271, 179, 151
10′	**19**	(iso)rhamnetin-3-*O*-hexoside	478	60.3	354, 264 (sh), 350	477[b]	315[d], 314[j]	301, 300, 285, 271, 257, 243
11′	**20**	kaempferol-3-*O*-pentoside	418	61.1	264, 346	417[b]	285[i], 284[k]	255, 227
12′	**21**	kaempferol-3-*O*-deoxyhexoside	432	65.7	264, 344	431[b]	284[l]	255, 239, 227

[a][2M − H]$^-$. [b][M − H]$^-$. [c][M − H + C_2H_2O]$^-$. [d][M − H-hexose]$^-$. [e][M − H-C-hexose]$^-$. [f][M − H-2x-C-hexose]$^-$. [g][M − H-(deoxyhexose +hexose)]$^-$. [h][M − H-(deoxyhexose+hexose)-CH_3]$^-$. [i][M − H-pentose]$^-$. [j][M − H-hexose]$^•$. [k][M − H-pentose]$^•$. [l][M − H-deoxyhexose].

3. RESULTS AND DISCUSSION

Dementia pathologies such as Alzheimer's disease (AD) are reaching epidemic proportions, yet they are not successfully managed by effective symptomatic treatments. Apoptosis and oxidative stress seemed to be involved in AD initiation, promotion, and progression. The search of formulations able to modulate these processes has led to the identification of effective antioxidant natural plant preparations (plant extracts and/or pure substances). Promising findings obtained may constitute a basis for alternative future neuroprotection strategies. In this context, the definition of the neuroprotective value of a *Laurus nobilis* leaf alcoholic extract and of its derived active fractions was of interest.

3.1. Metabolic Profiling and Fractionation of Alcoholic Parental Extract from *L. nobilis* Leaves. The biochemical complexity of the alcoholic parental extract did not lead to a direct and comprehensive identification of all its phytochemical constituents: a weak presence of terpene and allylphenol metabolites was detected by GC-MS,[13] whereas LC-MS/MS techniques allowed for insight into the abundant phenolic compound spectrum of the extract. In order to obtain a qualitative scenario of the real phytochemical composition of the plant complex, different fractionation procedures were applied allowing the establishment of extracts strongly dissimilar in terms of polarity and solubility of their constituents (Figure 1). Through liquid−liquid extraction techniques, an aqueous (LnM-1) and an organic fraction (LnM-2) were obtained. The aqueous fraction (LnM-1), which was enriched with highly polar or water-soluble constituents, was further fractionated using the XAD nonionic macroporous resins with a polystyrene-divinyl benzene copolymer matrix (XAD-4) and acrylic ester polymer (XAD-7); H_2O and MeOH were used as eluents. The use of polymers with hydrophobic properties allowed us to obtain an aqueous fraction (LnM-1a) and an organic fraction (LnM-1b). The organic fraction (LnM-2) was further separated through SiO_2 CC. The elution, carried out using three organic solvents with increasing polarity ($CHCl_3$, EtOAc, and MeOH), allowed us to obtain LnM-2a, LnM-2b, and LnM-2c fractions.

3.2. LC-MS/MS Based Metabolic Fingerprinting of Laurel Leaf Polar Fractions. The chromatographic profiles of the MeOH extract (LnM) and its fractions LnM-1, LnM-1a, LnM-1b, and LnM-2c (Figure 2), acquired at 280 and 300 nm, showed similar compound profiles. The only exception was LnM-1a, in which phenolics appeared to be absent. The structures of the main metabolites identified and LC-MS/MS and UV spectral data are reported in Figure 3 and in Table 1, respectively.

The complete overlapping of the metabolic profiles of the LnM-1 and LnM-1b extracts allows us to refer representatively

dx.doi.org/10.1021/tx5000415 | Chem. Res. Toxicol. 2014, 27, 611−626

to the characterization of extract LnM-1b, in which 10 different compounds were identified. Compound **1** was identified as a hexoside of 3,4-dihydroxybenzoic acid, e.g., protocatechuic acid, previously reported as a constituent of laurel leaf extracts.[22] The $[M - H]^-$ and the corresponding deprotonated dimer $[2M - H]^-$ were detected at m/z 315 and 631, respectively. The MS^2 spectrum of $[M - H]^-$ yielded three fragments of which m/z 153, resulting from the loss of a hexose, was the most abundant. The isolation of this ion and its dissociation yielded an ion of the second generation (MS^3) at m/z 109, likely due to the loss of CO_2 (44 Da) representing the carboxyl function of the 3,4-dihydroxybenzoic acid. Compound **2** was tentatively identified as 2′,*β* -dihydroxy-*α*,*β*-dihydrochalcone-*α*-*O*-hexoside. The UV spectrum showed the maximum absorption at 298 nm. The deprotonated ion m/z 419 and a low fragment ion at m/z 285 were probably due to the 1,5-type of cross-ring cleavage in a hexose sugar ring.[23] In MS^2, the neutral loss of 162 Da, confirmed the presence of a *O*-hexosyl moiety. The collision of the fragment ion at m/z 257 generated the fragment ion at m/z 221, whose formation could be due to the dehydration of the precursor ion at m/z 257 yielding a *β*-hydroxychalcone, which underwent a cyclization reaction involving the nucleophilic attack of the hydroxyl function on C-2′ at the C-*β* carbon. The MS spectrum of compound **3** allowed us to hypothesize the presence of an *O*-hexosyl of the 1-(2′-hydroxyphenyl)-3-phenylpropan-1,2-diol. The deprotonated ion $[M - H]^-$ was detected at m/z 451. The formation of a product ion at m/z 405 through the loss of 46 Da suggested that the observed molecular ion corresponded to a formic acid adduct $[M - H + CH_2O_2]^-$. The ion at m/z 405 underwent elimination of a hexose, to yield an ion at m/z 243, which dehydrated into the corresponding 2′-hydroxy-*α*,*β*-dihydrochalcone furnishing the fragment ion at m/z 225.

The UV spectrum, which showed a discrete maximum at 292 nm, and the mass spectrum of the metabolite corresponding to compound **4** suggested the presence of a coumaric acid hexoside.[24] In fact, the MS^2 experiment of m/z 325 yielded two fragment ions at m/z 163 and 119. The first one corresponded to the deprotonated coumaric acid through the loss of a hexose moiety, while the fragment at m/z 119 was due to a rearrangement with the loss of carbon dioxide. Compound **5** was tentatively identified as the *O*-hexosyl of *α*,2′-dihydroxy-*α*,*β*-dihydrochalcone. After fragmentation of the eluent adduct ion $[M - H + CH_2O_2]^-$ at m/z 449, the collision of the product ion at m/z 403 yielded m/z 241 (loss of a hexose), m/z 223 (loss of water), and m/z 179.

MS^n spectra of compound **6** were in accordance with the presence of a bis-C-glycosylated flavone. The MS spectrum exhibited the deprotonated molecule at m/z 593, which produced MS^2 ions at m/z 575 $[M - H-18]^-$, 503 $[M - H-90]^-$, and 473 $[M - H-120]^-$ (base peak). The losses of 90 and 120 Da allowed us to hypothesize the presence of a hexose residue linked to a flavonoid by a C–C bond.[25] Further collision of the ion at m/z 473 yielded m/z 353 (loss of 120 Da) indicating the presence of a second *C*-hexosyl moiety. The fragment ion at m/z 383 [aglycone + 113] allowed us to identify the aglycone as the flavone apigenin.[26] As C-linked saccharide residues were found only in the C-6 and/or C-8 positions of flavone skeletons, compound **6** was assigned as apigenin-6,8-di-C-hexoside.[27,28]

Mass spectrometric analysis of compound **7** was in accordance with the presence of a *C*-glycosyl flavone with a further O-glycosylated sugar attached. In fact, the fragmentation of the pseudomolecular ion m/z 577 led to the formation of m/z 457 $[M - H - 120]^-$, characterizing the hexosyl moiety from C-glycosylation,[25] and a fragment at 413 m/z ($[M - H - 164]^-$). This latter was formed by the scission of a deoxyhexose moiety from O-glycosylation on the hydroxyl group at position 2 of the 6-C-glycosylated sugar.[29,30] The presence of fragment ions at m/z 341 [aglycone + 71]$^-$ and m/z 293 [aglycone + 41 − 18]$^-$, usual in mono-*C*-glycosyl derivatives O-glycosylated on C-2″,[30] allowed us to tentatively identify compound **7** as 2″-*O*-deoxyhexosyl-C-hexosyl apigenin.

The UV spectrum, which showed two absorption bands at 256 and 354, relating to the conjugations in the B and A rings of a flavonoid aglycone, respectively, and the mass spectrum of compound **8** were in accordance with the presence of quercetin-3-*O*-(6″-*O*-deoxyhexosyl)-hexoside.[31] In fact, the MS^2 spectrum of the deprotonated molecular ion $[M - H]^-$ at m/z 609 generated the ion $[M - H-C_6H_{10}O_5-C_6H_{11}O_4]^-$ at m/z 301, representing the flavonol quercetin, corresponding to the loss of a disaccharide hexose-deoxyhexose moiety (162 + 146 Da). The $[Aglycone-H-CO-H]^-$ ion at m/z 271 and the $[aglycone-H-CO_2-H]^-$ ion at m/z 255 were observed in the $[aglycone-H]^-$ product ion spectrum suggesting that glycosylation occurred at the C-3 position.[32] Metabolites **9** and **10** were assigned as kaempferol-3-*O*-(6″-*O*-deoxyhexosyl)-hexoside and (iso)rhamnetin-3-*O*-(6″-*O*-deoxyhexosyl)-hexoside, respectively, on the basis of the absorbance bands of the UV–vis spectrum and mass spectrometric experiments and correspondence with previously published data.[29,33] The glycosylation position was assigned to be at hydroxyl group on C-3 carbon of both the flavonol aglycones on the basis of their characteristics fragmentation. In fact, the $[aglycone-H]^-$ (m/z 285) product ion spectrum of compound **9** showed an abundant $[aglycone-CO]^-$ ion at m/z 257, whereas the collision of the (iso)rhamnetin deprotonated ion at m/z 315 from **10** generated, besides the fragment ion at m/z 300 (due to the methyl residue loss), ions at m/z 271 and 255.

HPLC-DAD-ESI-MS^n analysis of the LnM-2c extract allowed the identification of 13 compounds, 2 of which (**9** and **10**) were already observed in LnM-1b (Table 1 and Figure 3).

Compound **11** was tentatively identified as the proanthocyanidin cinnamtannin B1, previously reported as the constituent of the aqueous infusion of laurel leaves.[22] The mass spectrum showed the peak of the deprotonated molecule at m/z 863. The MS^2 spectrum of the precursor ion showed a fragment at m/z 711 due to a retro-Diels–Alder fragmentation. The loss of 152 Da suggested that the terminal unit was (epi)catechin.[34] A further loss of 152 Da promoted the formation of an ion at m/z 559. The presence of the monomer (epi)catechin was evidenced from the fragment at m/z 289. The absorption bands at 268 and 338 nm for compound **12** and information provided by the MS^2 spectrometry experiments are consistent with the presence of a C-hexosyl apigenin. In fact, the deprotonated molecular ion $[M - H]^-$ at m/z 431 generated two fragment ions at m/z 341 [aglycone + 71]$^-$ and 311 [aglycone + 41]$^-$ characterizing the aglycone apigenin.[30] The localization of the sugar at C-8 is dictated by the loss of a single residue of carbon monoxide from the ion at m/z 311 as a consequence of the cross-ring cleavage of the six terms saccharide residue, with formation of an ion with m/z 283.[35] The presence of the aglycone apigenin was further confirmed by the m/z 117 ion in the MS^3 spectrum due to the characteristic apigenin retro-Diels–Alder fragmentation.[29]

dx.doi.org/10.1021/tx5000415 | Chem. Res. Toxicol. 2014, 27, 611–626

Compound **13** was tentatively identified as tetramethoxydihydroquercetin-3-*O*-pentoside. The fragmentation of the deprotonated molecular ion at m/z 491 yielded an m/z of 359 $[M - H{-}C_5H_9O_4]^-$, attributable to the aglycone and indicative of the loss of a pentose (132 Da). The formation of the ions of the second and third generation at m/z 344 (loss of 15 Da) and 329 (15 Da), respectively, confirmed the presence of methyl residues.

Compounds **14** and **15** were tentatively identified as two isomers of quercetin hexoside. The MS spectrum of compound **14** showed the deprotonated molecular ion at m/z 463, which provided an abundant radical aglycone product ion (m/z 300) and $[aglycone{-}H]^-$ fragment at m/z 301. The formation of the radical $[aglycone{-}H]^{\bullet -}$ is due to a homolytic cleavage of the aglycone−sugar bond. This radical breaking of the *O*-glycoside flavonoids resulting in a aglycone product with an odd number of electrons was previously addressed.[36] The MS^3 spectrum of the $[aglycone{-}H]^-$ provided the fragment ions at m/z 271 and 255 suggesting that glycosylation was at the C-3 position.[32] It was previously reported that the formation of the aglycone radical appears to be strongly correlated with the antioxidant activity of flavonoids. It was observed that its abundance for flavones and flavonols depends on the pattern of hydroxylation of the B ring and by the nature and the position of the saccharide residues.[36] The collision of the $[M - H]^-$ (m/z 463) gave, for compound **15**, the aglycone product ion at m/z 301. The $[aglycone{-}H{-}CO{-}H]^-$ ion at m/z 271 was, also in this case, observed suggesting that the hexose residue is located at 3-*O*-position. The MS^3 experiment allowed us to observe, again, the formation of characteristic quercetin fragment ions. The mass spectrum of **16** was in accordance with the presence of a quercetin-3-*O*-pentoside. In fact, it showed the deprotonated molecular ion $[M - H]^-$ at m/z 433 and the corresponding dimeric deprotonated ion $[2M - H]^-$ at m/z 867. The collision of the ion $[M - H]^-$ generated a radical aglycone m/z 300 as the main peak and a fragment ion at m/z 301 pointing to the flavonol quercetin. The neutral loss of 132 Da suggested the pentose nature of the glyconic moiety.

The collision of the ion $[M - H]^-$ relative to the metabolite **17** (m/z 447) provided an aglycone radical m/z 284, as well as the ion at m/z 285, attributable to the flavonol kaempferol. The loss of a fragment of 162 Da suggested the presence of a hexose sugar. The UV spectrum, which showed two absorption bands at 256 and 348 nm, and the data provided by MS/MS experiments suggested **18** to be quercetin-3-*O*-deoxyhexoside. Indeed, the dissociation of the ion $[M - H]^-$ yielded m/z 301, identifiable in the deprotonated quercetin, with a loss of a fragment of 146 Da, commonly attributed to the presence of a deoxyhexose unit. Compound **19** was putatively assigned as (iso)rhamnetin-3-*O*-hexoside. The collision of the ion $[M - H]^-$ at m/z 477 provided the radical aglycone at m/z 314, as well as the deprotonated aglycone (m/z 315), pointing to the flavonol isorhamnetin. The presence of the methyl derivate of quercetin was further confirmed, in the MS^3 spectrum, from the fragment ions at m/z 301 and 300.

The UV−vis spectral data and those derived from tandem mass spectrometry experiments suggested that metabolites **20** and **21** were kaempferol-3-*O*-pentoside and kaempferol-3-*O*-deoxyhexoside, respectively. In the spectra of both the molecules, the presence of kaempferol was elicited through the formation of the relative aglycone radical (m/z 284) with losses of a glycone radical of 133 Da for compound **20** and of a glycone radical of 147 Da for compound **21**.

Our findings are in accordance with data reported by Ayoub et al.[37] who isolated several active flavonol ingredients from an hepatoprotective laurel leaf extract. Glycosides of kaempferol, quercetin, and isorhamnetin were the main constituents of the extract. Rhamnose, glucose, galactose, and rutinose were identified as sugar moieties. The isolation of antibacterial acylated kaempferol derivatives from laurel leaves was also described.[38]

3.3. Antioxidant Activity of the LnM Extract from *Laurus nobilis* Leaves.

In order to evaluate the antioxidant capacity of the MeOH parental extract (LnM) and its fractions, several assays were set up to verify its role as the scavenger of radical species by transfer of a hydrogen atom or a single electron (Table 2 and Figure 4).

Table 2. DPPH and ABTS ID_{50} (μg/mL) Values[a]

				Trolox (μM equiv)		
	DPPH$^\bullet$ ID_{50} (μg/mL)	$ABTS^{+\bullet}$ ID_{50} (μg/mL)	ROO$^\bullet$ ID_{50} (μg/mL)	1.0 μg/mL	2.5 μg/mL	5.0 μg/mL
LnM	21.5	8.6	>5.0	5.0	8.2	9.2
LnM-1	21.9	9.7	>5.0	4.3	5.2	5.8
LnM-2	10.8	1.8	3.0	6.8	10.1	14.5
LnM-1a	>100.0	>100.0	>5.0	2.0	2.3	3.4
LnM-1b	14.5	3.7	2.6	6.2	11.2	15.0
LnM-2a	>100.0	37.0	>5.0	3.5	4.9	8.6
LnM-2b	5.9	0.5	1.6	8.5	14.6	17.3
LnM-2c	11.8	0.9	1.7	8.8	13.8	16.9

[a]ROO$^\bullet$ ID_{50} (μg/mL) from ΔAUC values and Trolox (μM) equivalents from the ORAC test.

As is clear from Table 2, the LnM extract showed an effective reducing power of the radical species target $ABTS^{\bullet+}$ and DPPH$^\bullet$, quantifiable in the respective ID_{50} values (8.6 μg/mL vs the ABTS radical cation and 21.5 μg/mL vs the DPPH radical). The scavenging effectiveness seemed to be strongly dependent on the tested dose: the ABTS radical cation was completely converted in its reduced form at 25.0 μg/mL dose. The massive antiradical activity, attributable, as evidenced by LC-MS/MS analysis, to the conspicuous presence of flavonoid molecules, was further confirmed by the results of the ORAC test, a test that measures the HAT oxidative degradation of fluorescein by peroxyl radicals with the formation of a nonfluorescent product, which can be easily quantified by spectrofluorimetric measurements.[39] To obtain useful information, the high sensitivity of the ORAC method required the use of lower doses of extract than those adopted in the colorimetric tests (1.0, 2.5, and 5.0 μg/mL). When the superoxide anion radical scavenging activity was tested, it was observed that the extract was able to inhibit the synthesis of the ROS species in the assay medium in a dose-dependent manner eliciting an ID_{50} value equal to 6.0 μg/mL. As the 2-deoxyribose oxidation plays a crucial role in genetic toxicology of oxidative stress beyond the recombinant consequences of single- and double-strands breaks, the LnM OH$^\bullet$ scavenging effects were evaluated. Obtained data highlighted that the extract was active vs OH radicals when tested doses were greater than 25.0 μg/mL. At the highest tested dose, LnM scavenged efficiently by 65%. The antiradical activity was not clearly shown when NO radical scavenging assay was performed: a weak nitric oxide scavenging ability was detected in all the range of doses tested.

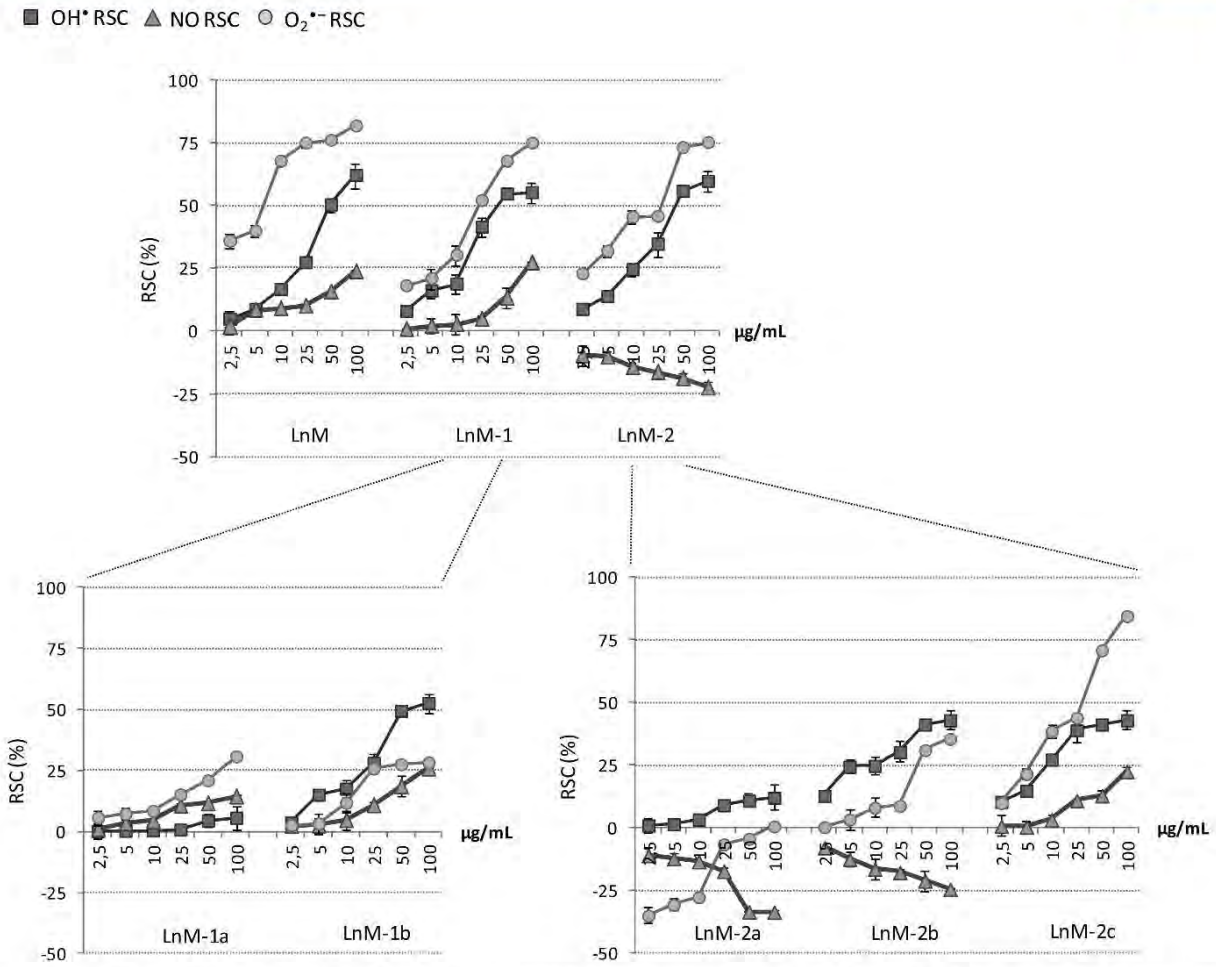

Figure 4. Radical scavenging capacity (RSC, %) of *L. nobilis* investigated extracts toward OH• radical, $O_2^{\bullet -}$, and NO. Values, reported as percentage vs a blank, are the mean ± SD of measurements carried out on 3 samples (n = 3) analyzed three times.

3.4. Antioxidant Activity of LnM-Derived Fractions. Upon comparison of scavenging effectiveness of LnM and its polar fractions LnM-1a, LnM-1b, and LnM-2c, it could be stated that the aqueous fractions, further enriched in polar and water-soluble constituents, were less active than the parental extract. In particular, LnM-1a, deprived of the components belonging to secondary metabolism, exhibited a very weak scavenging activity so as to render impossible the ID_{50} calculation. On the contrary, alcoholic extracts, LnM-1b, and LnM-2c were able to exert an activity more effective than the parental extract, confirming that the strong presence of inert components, such as sugars, could mask the bioactivity of secondary metabolites constituting the plant drug. Although the two alcohol fractions were responsible for a marked radical scavenging capacity, LnM-2c seemed to exert antiradical effects stronger than that of LnM-1b. LnM-2c ID_{50} values were equal to 11.8 and 0.96 μg/mL vs the DPPH radical and ABTS radical cation, respectively. Similarly, differences highlighted by the ORAC test were evident: LnM-2c showed a marked delay in the fluorescein decay curve. Both the extracts were unable to scavenge nitric oxide but showed a dissimilar behavior toward the ROS species used as targets. In fact, LnM-2c showed an important reduction of the superoxide anion radical, whereas LnM-1b was active in counteracting OH radicals synthesis.

The assessment of the radical scavenging ability of the LnM-2, LnM-2a, and LnM-2b extracts evidenced the strong efficacy of the LnM-2 extract and its LnM-2b fraction. Indeed, the LnM-2 extract was able to powerfully scavenge all of the tested radicals exhibiting ID_{50} values equal to 10.8 μg/mL vs the DPPH, 1.8 μg/mL vs the ABTS radical cation, 3.0 μg/mL vs ROO•, 50.5 μg/mL vs OH•, and 16.9 μg/mL vs $O_2^{\bullet -}$. Upon the fractionation of the LnM-2 extract, it was observed that among the apolar fractions obtained, only LnM-2b retained high antiradical activity especially toward DPPH•, $ABTS^{+\bullet}$, and ROO•. Nevertheless, LnM-2 and its apolar fractions were able to induce NO production in the assay medium.

3.5. Cytotoxic Effects of the LnM Extract from *Laurus nobilis* Leaves. MTT and SRB tests were employed to assess laurel leaf extract efficacy. As shown in Table 3, data from the SRB assay correlated well with those of the MTT assay, although calculated ID_{50} values were slightly higher from SRB than from MTT. This finding is in accordance with the ability of MTT to detect only viable cells, whereas the SRB method does not distinguish between viable and dead cells.[40] The cytotoxic capacity of the extract was time- and dose-dependent on the three tested cell lines. The rat cells (C6) were shown to be less sensitive to the addition of the extract: a very weak inhibition of cell viability at all three exposure times considered

dx.doi.org/10.1021/tx5000415 | Chem. Res. Toxicol. 2014, 27, 611−626

Table 3. MTT and SRB ID_{50} (μg/mL) Values of the LnM Extract from *Laurus nobilis* and Fractions Therefrom[a]

		MTT ID_{50} (μg/mL)			SRB ID_{50} (μg/mL)		
		24 h	48 h	72 h	24 h	48 h	72 h
SK-N-BE(2)-C	LnM	126.5	54.9	49.1	>250.0	>250.0	>250.0
	LnM-1	>250.0	>250.0	>250.0	>250.0	>250.0	>250.0
	LnM-2	37.7	38.4	37.2	>250.0	23.1	14.4
	LnM-1a	>250.0	>250.0	>250.0	>250.0	>250.0	>250.0
	LnM-1b	>250.0	>250.0	>250.0	>250.0	>250.0	>250.0
	LnM-2a	14.0	14.6	18.5	>250.0	22.9	13.1
	LnM-2b	60.6	54.4	48.7	>250.0	35.9	28.1
	LnM-2c	>250.0	>250.0	>250.0	>250.0	>250.0	>250.0
SH-SYSY	LnM	50.3	56.0	33.0	57.4	55.2	50.4
	LnM-1	>250.0	>250.0	>250.0	>250.0	>250.0	>250.0
	LnM-2	41.2	42.8	39.5	26.7	26.0	23.0
	LnM-1a	>250.0	>250.0	>250.0	>250.0	>250.0	>250.0
	LnM-1b	>250.0	>250.0	>250.0	>250.0	>250.0	>250.0
	LnM-2a	23.3	17.5	17.0	23.4	21.6	20.4
	LnM-2b	>250.0	>250.0	>250.0	43.4	40.8	35.4
	LnM-2c	>250.0	>250.0	>250.0	>250.0	>250.0	>250.0
C6	LnM	>250.0	>250.0	240.6	>250.0	>250.0	>250.0
	LnM-1	>250.0	>250.0	>250.0	>250.0	>250.0	>250.0
	LnM-2	>250.0	216.8	104.3	>250.0	>250.0	>250.0
	LnM-1a	>250.0	>250.0	>250.0	>250.0	>250.0	>250.0
	LnM-1b	>250.0	>250.0	>250.0	>250.0	>250.0	>250.0
	LnM-2a	31.1	30.5	30.0	42.8	41.2	33.0
	LnM-2b	>250.0	134.0	59.8	>250.0	235.0	86.8
	LnM-2c	>250.0	>250.0	>250.0	>250.0	>250.0	>250.0

[a]The ID_{50} value was calculated on the basis of cell viability inhibition data towards SK-N-BE(2)-C, SH-SY5Y, and C6 cell lines at 24 h, 48 h, and 72 h of exposure times. The measurements were carried out on 3 samples (n = 3) analyzed 12 times.

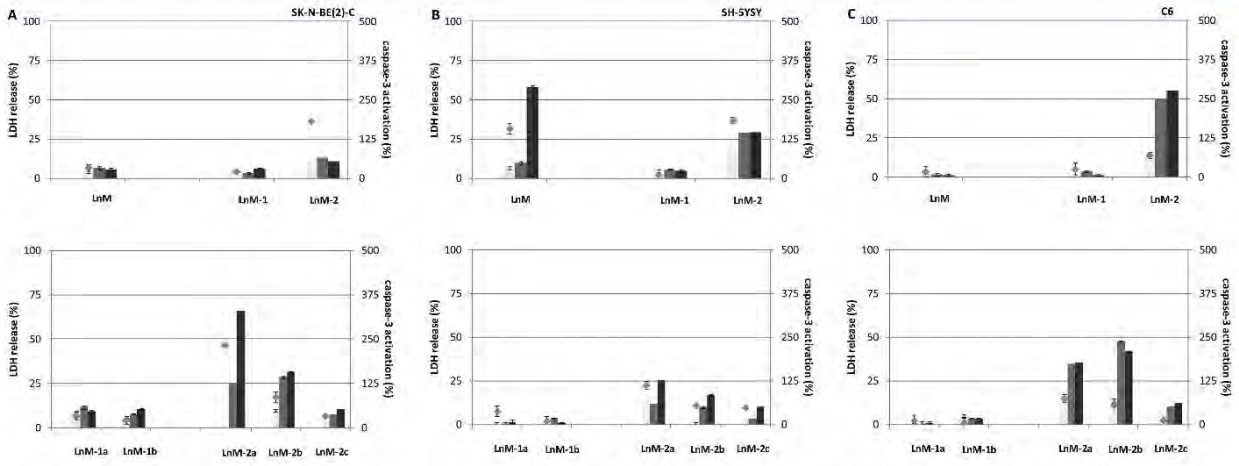

Figure 5. LDH release (±SD) and caspase-3 activation (±SD) of (A) SK-N-BE(2)-C cell line, (B) SH-SY5Y cell line, and (C) C6 cell line. The evaluation of LDH release was carried out treating cells with a 100.0 μg/mL extract dose at 24 h, 48 h, and 72 h exposure times. The evaluation of caspase-3 activation was carried out treating cells with a 100.0 μg/mL extract dose at the 48 h exposure time. Values, reported as percentage vs an untreated control, are the mean ± SD of measurements carried out on 3 samples (n = 3) analyzed 12 times.

was observed. C6 cells as a key modulator of neuroprotection are generally less susceptible to cytotoxic or ROS generating substances because of high glutathione (GSH) content.[41] When the doses 100.0 and 250.0 μg/mL were added, only at 72 h of exposure time, a significant antiproliferative effect on murine cells was recorded. Cell viability was inhibited by 60−98% and 80−90% in the MTT assay and SRB, respectively. Thus, the exposure of the glial cells to increasing doses of extract caused mild but dose- and time-dependent cytotoxic effects. These effects were not comparable to the toxicity exerted on the other two tested cell lines which instead have a responsive capacity similar to that of the extract, at the highest dose tested, for all the three exposure times (24, 48, and 72 h) was about 97% for the cells SK-N-BE-(2)-C and 93% for the SH-SY5Y cells.

In order to investigate the mechanism that underlies the cell viability inhibition exerted by LnM, the effect on the plasma membrane integrity by the lactate dehydrogenase (LDH) assay and on the activation of caspase-3, an effector of apoptosis, was quantified using a dose of 100.0 μg/mL, at which the extract exhibited a clear cytotoxic effect on all of the tested cell lines.

dx.doi.org/10.1021/tx5000415 | Chem. Res. Toxicol. 2014, 27, 611−626

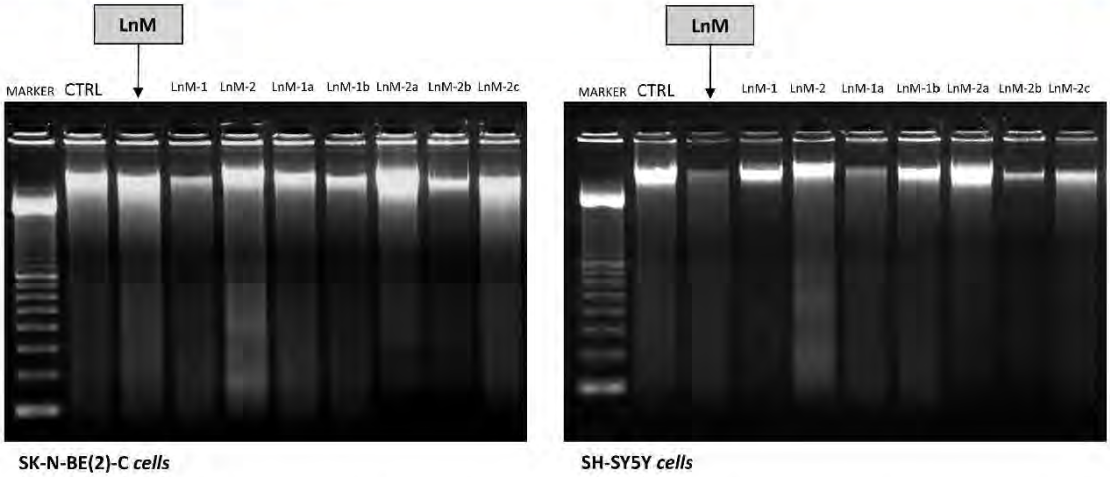

Figure 6. DNA fragmentation of SK-N-BE(2)-C (left) and SH-SY5Y (right) cells induced by *L. nobilis* extracts (LnM, LnM-1, LnM-2, LnM-1a, LnM-1b, LnM-2a, LnM-2b, and LnM-2c). Genomic DNA was isolated from all cell samples as described in Materials and Methods and analyzed by electrophoresis on 2% agarose gel stained with ethidium bromide. A comparison with the molecular weight marker indicated that bay leaf extracts cause a "ladder" pattern of DNA in treated cells and absence of DNA fragmentation in untreated cells. The panels show the results of one representative experiment out of three independent ones.

The extract was not able to determine a significant increase (compared to the control) of the release of enzyme LDH in the culture medium at 24 and 48 h of exposure times. As a key signature for necrotic cells is an increasing permeabilization of the plasma membrane,[42] which is accompanied by the release of the enzyme lactate dehydrogenase, detected data suggested to us that the observed inhibition of proliferation was not due to necrotic death (Figure 5). Death by necrosis could occur secondarily as a result of long exposure times. In fact, after 72 h of exposure, in SH-SY5Y cells enzyme LDH release percentage equal to 54% was observed.

When the caspase-3 activity was determined by measuring the release of the chromophore *p*-nitroaniline (*p*-NA), following the hydrolysis of the substrate DEVD-*p*-NA, operated by the same enzyme, it was observed that LnM induced weak apoptosis of the SH-SY5Y cell line (158%). Moreover, nontypical apoptotic DNA fragments were detected when a DNA fragmentation assay was performed (Figure 6). This finding does not contradict the quantitative data from the caspase-3 activation assay. In fact, it is known that the detectability of the DNA ladder assay can be decreased also in samples where the number of apoptotic cells is lower than about 5%.

2.6. Cytotoxic Effects of LnM-Derived Fractions. MTT and SRB cytotoxic data of aqueous (LnM-1 and LnM-1a) and alcoholic (LnM-1b and LnM-2c) phytoextracts are also reported in Table 3. The abundant presence of cytoprotective phenolic molecules and/or inert saccharides in the four polar fractions made them less cytotoxic than the parental extract. The LnM-1 fraction and the alcoholic extract derived therefrom showed a similar cytotoxic effect. Both the fractions were able to induce a decrease of cell viability of slightly above 30% at the highest doses tested in human cell lines. An inhibition percentage close to 50% and strongly time-dependent was also observed in the less sensitive murine cells. The LnM-1a extract, deprived of the polyphenolic component, was the least active. The LnM-2c fraction showed a cytotoxic profile strongly dependent on the cell line exposed to it. In fact, the extract was not cytotoxic toward the murine cell line. It was able to exert an inhibition percentage close to 25% across the range of tested doses on cells SK-B-NE(2)-C and a reduction of viability over 50% in the other human neuroblastoma cell line. The weak cytotoxic effect registered results in a weak LDH release and in a poor caspase-3 activation (Figure 5).

Contrariwise, LnM-2, LnM-2a, and LnM-2b plant extracts seemed to retain and/or enhance the cytotoxic effects shown from the parental extract (Table 3). The results of the MTT and SRB assays demonstrated that the LnM-2 phytoextract exerted cytotoxic effects (dose- but not time-dependent) similar to those produced from the parental extract on the murine cell line and effects far more pronounced, even at low doses, toward human neuroblastoma cell lines. Cytotoxicity was particularly high when the three cell lines were exposed to increasing doses of the LnM-2a ($CHCl_3$) fraction. In particular, it was observed that already a 50 μg/mL dose determined an inhibition of cell viability close to 100%. The marked activity was presumably due to the strong presence of sesquiterpenes, which, as reported in literature, are cell death inducers.[43]

The abundance of cytotoxic guaianolide-type sesquiterpenes made LnM-2a, as well as LnM-2, strong inducers of the apoptotic process. In fact, a higher percentage of the caspase-3 activation equal to 232% in SK-N-BE(2)-C was recorded. Using qualitative analysis of DNA fragmentation, we observed that a DNA ladder occurred (Figure 6).

3.7. Effect of the LnM Extract and Its Fractions on Aβ(25−35)- and H_2O_2-Mediated Cytotoxicity. It has been reported that Aβ impairs mithocondrial redox activity increasing the generation of reactive nitrogen and oxygen species.[8] In order to evaluate the possible beneficial effect of the parental extract and its fractions in neuronal death by oxidative stress induced by amyloid plaques in Alzheimer's dementia, the antioxidant capacity of these extracts were tested in an *in vitro* system utilizing the functional domain of the β-amyloid peptide.

As the cellular reduction of MTT represents a specific indicator of the initial events underlying the mechanism of β-amyloid peptide toxicity,[44,45] the MTT test was first carried out exposing the three cell lines at increasing concentrations of the

dx.doi.org/10.1021/tx5000415 | *Chem. Res. Toxicol.* 2014, 27, 611−626

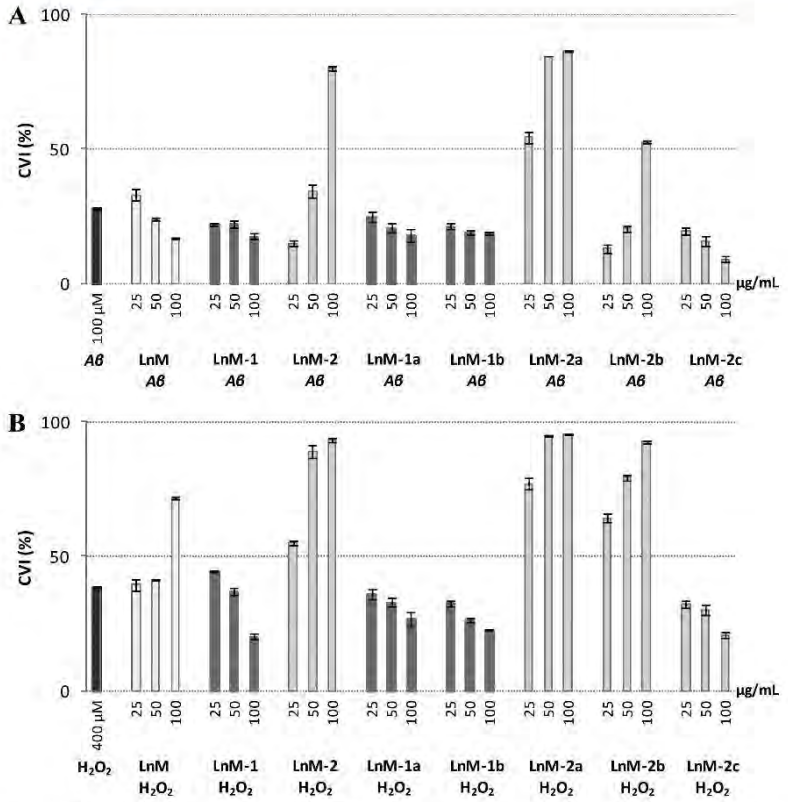

Figure 7. Cell viability inhibition (CVI, %) toward SK-N-BE(2)-C and SH-SY5Y cotreated with LnM and its fractions and the (A) Aβ(25−35) fragment. (B) H_2O_2 (400 μM) at 24 h exposure time by means of MTT test results. Values, reported as percentage vs an untreated control, are the mean ± SD of measurements carried out on 3 samples (n = 3) analyzed 12 times.

Aβ(25−35) fragment (12.5, 25.0, 50.0, and 100.0 μM). The Aβ(25−35) fragment was found to induce cytotoxicity in the SK-N-BE-(2)-C cell line. Thus, in order to evaluate the neuroprotective properties of laurel leaf extracts, the SK-N-BE-(2)-C cell line was pretreated for 24 h with 100.0 μM Aβ(25−35) and increasing doses (25.0, 50.0, and 100.0 μg/mL) of investigated extracts. The effects of the pretreatment were assessed again by running the MTT test. As can be seen from the graph shown in Figure 7A, the effects on Aβ-mediated cytotoxicity were strongly related to the metabolic composition of the tested extracts. In fact, the pretreatment with the parental extract rich in polyphenolic antioxidants, at doses of 25.0 and 50.0 μg/mL, seemed to favor a significant decrease in responsiveness of the adopted cellular system to the oxidant action. The extract appeared to exert a weak pro-oxidant effect at the highest dose tested. A null effect was attributable to the aqueous fractions and, in particular, to the phytoextract LnM-1a. The simultaneous addition of the oxidizing agent and the LnM-1a phytoextract detected the inertia of the molecules that characterize it. Alcoholic extracts LnM-1b and LnM-2c were the most effective at counteracting the oxidizing action of the amyloidogenic fragment. The high antioxidant capacity of LnM-2c, already proved with antioxidant screening in the test tube, was associated with an important highly dose-dependent cytoprotective effect.

LnM-2 and LnM-2b exhibited a behavior similar to that shown by the parental extract. In fact, they exerted a pro-oxidant effect markedly more pronounced at a dose equal to 100.0 μg/mL. Moreover, the $CHCl_3$ fraction seemed unable to counteract the cytotoxic activity of the Aβ(25−35) fragment. The results of the MTT assay suggested the exercise of a negative synergistic effect resulting from the summation of the Aβ and LnM-2a extract toxicities.

A similar behavior was observed when, in place of the Aβ(25−35) fragment, hydrogen peroxide was used as oxidizing agent. In fact, Figure 7B shows that the cotreatment of the cell line with the ROS species and extracts that did not exhibit cytotoxic effects favored the exercise of a protective effect which became gradually more significant with the increase of the dose tested. The copresence of the oxidizing agent and extracts as LnM-2a and LnM-2b led to a massive decrease in cell viability already at the lowest dose tested.

3.8. Effect of LnM and Its Fractions on Intracellular ROS Generation. In order to examine whether *Laurus nobilis* extracts can inhibit and/or prevent ROS generation induced by the known free radical generator hydrogen peroxide, the SK-N-BE-(2)-C cell line was incubated with the investigated extracts and H_2O_2 (400 μM). The assay was performed for 6 h, and the DCF fluorescence formation was determined by taking data every hour. The addition of LnM laurel leaf extract and its aqueous (LnM-1) and organic (LnM-2) fractions massively reduced the percentage of ROS formation in a time-exposure-dependent manner. When the LnM-1-derived extracts were screened, it was observed that the aqueous extract (LnM-1a) was highly inefficacious to counteract ROS formation, whereas the LnM-1b extract showed a ROS inhibiting activity comparable to that exerted by the parental extract. Analogously different antioxidant responses were from LnM-2-derived

dx.doi.org/10.1021/tx5000415 | *Chem. Res. Toxicol.* 2014, 27, 611−626

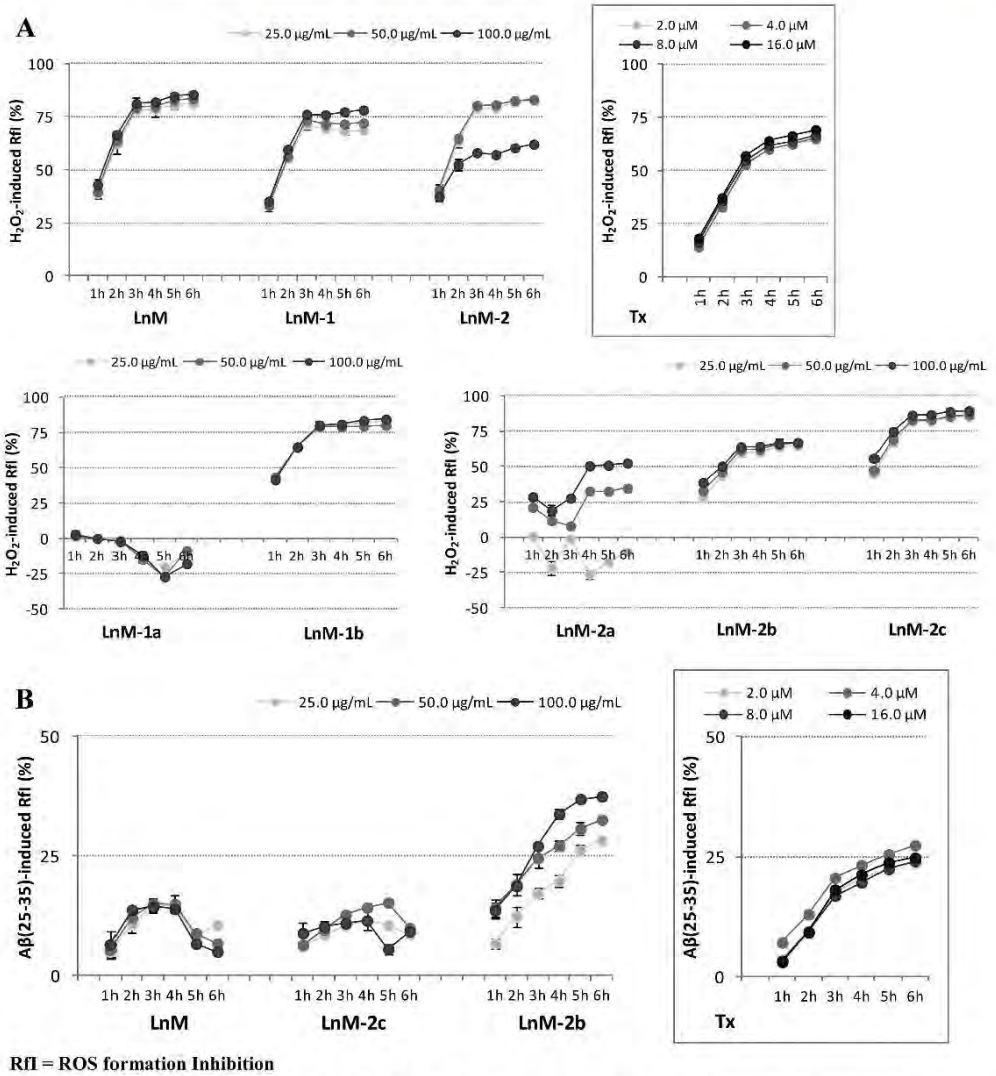

Figure 8. (A) Effect of *L. nobilis* extracts (LnM, LnM-1, LnM-2, LnM-1a, LnM-1b, LnM-2a, LnM-2b, and LnM-2c) and Trolox on H_2O_2-induced ROS generation in SK-N-BE(2)-C cells. (B) Effect of LnM, LnM-2a, and LnM-2c extracts and Trolox on Aβ(25−35)-induced ROS generation in SK-N-BE(2)-C cells. Rfl = ROS formation inhibition. Values, reported as percentage vs the oxidized control, are the mean ± SD of measurements carried out on 3 samples (n = 3) analyzed 12 times.

extracts. In particular, the LnM-2c fraction was able to inhibit ROS production by 56% at the highest tested dose level already after 1 h of exposure. The antioxidant potential was far greater than that exerted by Trolox, a known synthetic antioxidant compound, which was reported as a neuroprotective agent able to partially prevent Aβ-mediated toxicity and to decrease Aβ-induced ROS levels.[46] This finding suggested that we should further screen the antioxidant potential of the LnM-2c extract in a cell system in which Aβ(25−35) was used as a free radical generator. The intracellular ROS accumulation resulting from Aβ(25−35) treatment in the SK-N-BE(2)-C cell line was significantly reduced in dose-dependent manner when cells were cotreated with the LnM-2c extract (Figure 8B).

3.9. LnM-2c Shows Promising Antiamyloidogenic Effect. As Congo red (CR) is a symmetrical sulfonated azo dye able to bind amyloid proteins, a CR staining solution containing high content of alcohol and free alkali was used in order to examine the increase and/or the decrease of amyloid deposits in SK-N-BE(2)-C cells cotreated with LnM-2a and LnM-2c extracts and the Aβ(25−35) fragment, in reference to a control which underwent the only Aβ(25−35) domain treatment. Stained samples were examined using polarized light microscopy (Figure 9). The treatment with LnM-2c caused significant decreases in the percentages of CR-positive SK-N-BE(2)-C cells without affecting cell viability. On the contrary, the exposure to LnM-2c resulted in an increase of amyloid β-protein accumulation and cytotoxicity.

The preparation of extracts rich in flavonoid constituents could represent a valuable and alternative neuroprotection strategy. Previous research proved that flavonoids exert a multiplicity of neuroprotective actions within the brain, including a potential to protect neurons against injury induced by neurotoxins, an ability to suppress neuroinflammation, and the potential to promote memory, learning, and cognitive

dx.doi.org/10.1021/tx5000415 | *Chem. Res. Toxicol.* 2014, 27, 611−626

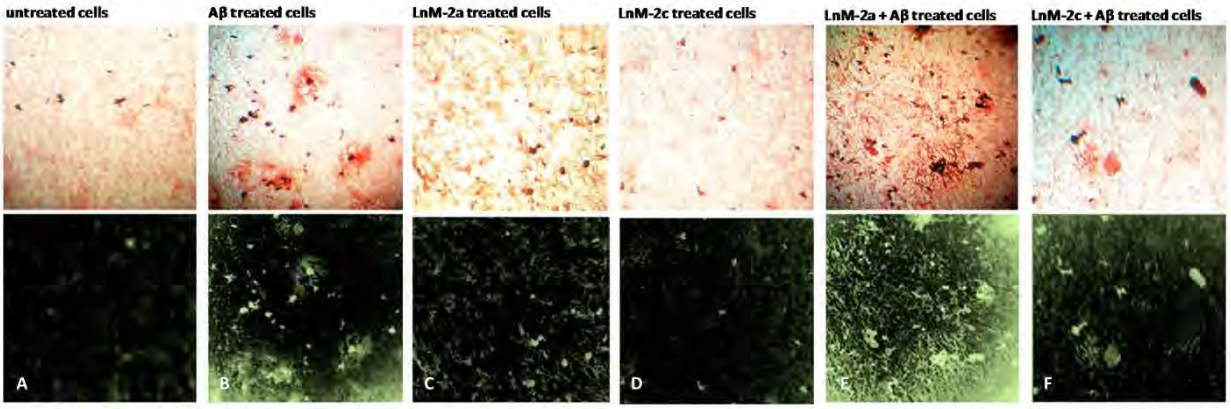

Figure 9. Congo red staining of the (A) untreated SK-N-BE(2)-C cell line; SK-N-BE(2)-C cell line treated with the (B) Aβ(25−35) fragment, (C) LnM-2a, (D) LnM-2c; SK-N-BE(2)-C cell line cotreated with (E) LnM-2a and Aβ(25−35) fragment, and (F) LnM-2c extracts and Aβ(25−35) fragment. Congo red staining was confirmed by green birefringence under polarized light. The panels show the results of one representative experiment out of three independent ones.

function.[47] A growing number of flavonoids have been shown to inhibit the development of AD-like pathology and to reverse deficits in cognition in rodent models, suggestive of potential therapeutic utility in dementia.[48] Different mechanisms have been suggested. The ability of flavonoids to delay the initiation of and/or slow the progression of AD-like pathology and related neurodegenerative disorders seemed be due to their potential to inhibit neuronal apoptosis triggered by neurotoxic species (e.g., oxidative stress) or disrupt amyloid β aggregation and effects on amyloid precursor protein processing through the inhibition of β-secretase (BACE-1) and/or activation of α-secretase (ADAM10). Together, these processes act to maintain the number and quality of synaptic connections in key brain regions. Thus, flavonoids have the potential to prevent the progression of neurodegenerative pathologies and to promote cognitive performance.

4. CONCLUDING REMARKS

As human life expectancy has increased, so has the incidence of age-related neurodegenerative disorders, such as Alzheimer's disease. The use of plant ingredients could be a valuable strategy to counteract neurodegeneration phenomena progress. In fact, plants contain a wide range of bioactive and health-promoting compounds. Phenol-rich extracts from *Laurus nobilis* leaves with pronounced antioxidant and antiamyloidogenic effects represent a promising alternative resource in Alzheimer's disease prevention and treatment. Our findings put down a foundation for further experiments in order to strengthen and clarify the ability of LnM-2c to inhibit Aβ-induced ROS formation.

AUTHOR INFORMATION

Corresponding Author

*Tel: +39 0823 274572. E-mail: severina.pacifico@unina2.it.

Funding

This work was supported by the Department of Environmental Biological and Pharmaceutical Sciences and Technologies of the Second University of Naples.

Notes

The authors declare no competing financial interest.

ABBREVIATIONS

ABTS, 2,2′-azinobis-(3-ethylbenzothiazolin-6-sulfonic acid); AD, Alzheimer's disease; AUC, area under curve; Aβ, amyloid β-protein; CR, Congo red; CVI, cell viability inhibition; DCFH-DA, 2′,7′-dichlorofluorescein diacetate; DMSO, dimethyl sulfoxide; DPPH, 2,2-diphenyl-1-picrylhydrazyl; ESI, electrospray ionization; EtOAc, ethyl acetate; EtOH, ethanol; ID_{50}, medium inhibition dose; INT, 2-(4-iodophenyl)-3-(4-nitrophenyl)-5-phenyltetrazolium chloride; LC MS, liquid chromatography−mass spectrometry; LDH, lactate dehydrogenase; LnM, *Laurus nobilis* methanolic extract; MeOH, methanol; MTT, 3-(4,5-dimethyl-2-thiazolyl)-2,5-diphenyl-2*H*-tetrazolium; MW, molecular weight; NBT, nitroblue tetrazolium; ORAC, oxygen radical absorbance capacity; *p*NA, *p*-nitroanilide; RfI, ROS formation Inhibition; RNS, reactive nitrogen species; ROS, reactive oxygen species; RSC, radical scavenging capacity; SD, standard deviation; SNP, sodium nitroprusside; SRB, sulforhodamine B; TBA, thiobarbituric acid; TCA, trichloroacetic acid

REFERENCES

(1) Mattson, M. P. (2004) Pathways towards and away from Alzheimer's disease. *Nature 430*, 631−639.

(2) Amtul, Z., Keet, M., Wang, L., Merrifield, P., Westaway, D., and Rozmahel, R. F. (2011) DHA supplemented in peptamen diet offers no advantage in pathways to amyloidosis: is it time to evaluate composite lipid diet? *PLoS One 6*, e24094.

(3) Tamango, E., and Guglielmotto, M. (2012) Amyloid-β production: major link between oxidative stress and BACE1. *Neurotoxic. Res. 22*, 208−219.

(4) Cai, Z., Zhao, B., and Ratka, A. (2011) Oxidative stress and β-amyloid protein in Alzheimer's disease. *Neuromol. Med. 13*, 223−250.

(5) Markesbery, W. R. (1997) Oxidative stress hypothesis in Alzheimer's disease. *Free Radical Biol. Med. 23*, 134−147.

(6) Floyd, R. A., and Hensley, K. (2002) Oxidative stress in brain aging. Implications for therapeutics of neurodegenerative diseases. *Neurobiol. Aging 5*, 795−807.

(7) Dok-Go, H., Lee, K. H., Kim, H. J., Lee, E. H., Lee, J., Song, Y. S., Lee, Y. H., Jin, C., Lee, Y. S., and Cho, J. (2003) Neuroprotective effects of antioxidative flavonoids, quercetin, (+)-dihydroquercetin and quercetin 3-methyl ether, isolated from *Opuntia ficus-indica* var. saboten. *Brain Res. 965*, 130−136.

(8) Kadowaki, H., Nishiton, H., Urano, F., Sadamitsu, C., Matsuzawa, A., Takeda, K., Masutani, H., Yodoi, J., Urano, Y., Nagano, T., and

Ichijo, H. (2005) Amyloid β induces neuronal cell death through ROS-mediated ASK1 activation. *Cell Death Differ. 12*, 19−24.
(9) Shi, C., Liu, J., Wu, F., and Yew, D. T. (2010) *Ginkgo biloba* extract in Alzheimer's Disease: from action mechanisms to medical practice. *Int. J. Mol. Sci. 11*, 107−123.
(10) Gupta, V. B., Indi, S. S., and Rao, K. S. J. (2009) Garlic extract exhibits antiamyloidogenic activity on amyloid-beta fibrillogenesis: relevance to Alzheimer's disease. *Phytother. Res. 23*, 111−115.
(11) Wang, J., Ho, L., Zhao, Z., Seror, I., Humala, N., Dickstein, D. L., Thiyagarajan, M., Percival, S. S., Talcott, S. T., and Pasinetti, G. M. (2006) Moderate consumption of Cabernet Sauvignon attenuates Abeta neuropathology in a mouse model of Alzheimer's disease. *FASEB J. 20*, 2313−2320.
(12) Ho, L., Yemul, S., Wang, J., and Pasinetti, G. M. (2009) Grape seed polyphenolic extract (GSE) as a novel therapeutic reagent in tau-mediated neurodegenerative disorders. *J. Alzheimer's Dis. 16*, 433−439.
(13) Pacifico, S., Gallicchio, M., Lorenz, P., Potenza, N., Galasso, S., Marciano, S., Fiorentino, A., Stintzing, F. C., and Monaco, P. (2013) Apolar *Laurus nobilis* leaf extracts induce cytotoxicity and apoptosis towards three nervous system cell lines. *Food Chem. Toxicol. 62*, 628−637.
(14) Prior, R. L., Wu, X., and Schaich, K. (2005) Standardized methods for the determination of antioxidant capacity and phenolics in foods and dietary supplements. *J. Agric. Food Chem. 53*, 4290−4303.
(15) Pacifico, S., D'Abrosca, B., Scognamiglio, M., Gallicchio, M., Potenza, N., Piccolella, S., Russo, A., Monaco, P., and Fiorentino, A. (2011) Metabolic profiling of strawberry grape (*Vitis* × *labruscana* cv. 'Isabella') components by NMR, and evaluation of their antioxidant and antiproliferative properties. *J. Agric. Food Chem. 59*, 7679−7687.
(16) Pacifico, S., Gallicchio, M., Fiorentino, A., Fischer, A., Meyer, U., and Stintzing, F. C. (2012) Antioxidant properties and cytotoxic effects on human cancer cell lines of aqueous fermented and lipophilic quince (*Cydonia oblonga* Mill.) preparations. *Food Chem. Toxicol. 50*, 4130−4135.
(17) Di Maro, A., Pacifico, S., Fiorentino, A., Galasso, S., Gallicchio, M., Guida, V., Severino, V., Monaco, P., and Parente, A. (2013) Raviscanina wild asparagus (*Asparagus acutifolius* L.): a nutritionally valuable crop with antioxidant and antiproliferative properties. *Food Res. Int. 53*, 180−188.
(18) Skehan, P., Storeng, R., Scudiero, D., Monks, A., McMahon, J., Vistica, D., Warren, J. T., Bokesch, H., Kenney, S., and Boyd, M. R. (1990) New colorimetric cytotoxicity assay for anticancer-drug screening. *J. Natl. Cancer Inst. 82*, 1107−1112.
(19) Muthaiyah, B., Essa, M. M., Chauhan, V., and Chauhan, A. (2011) Protective effects of Walnut extract against amyloid beta peptide-induced cell death and oxidative stress in PC12 cells. *Neurochem. Res. 36*, 2096−2103.
(20) Naval, M. V., Gómez-Serranillos, M. P., Carretero, M. E., and Villar, A. M. (2007) Neuroprotective effect of a ginseng (*Panax ginseng*) root extract on astrocytes primary culture. *J. Ethnopharmacol. 112*, 262−270.
(21) Linke, R. P. (2006) Congo Red Staining of Amyloid. Improvements and Practical Guide for a More Precise Diagnosis of Amyloid and the Different Amyloidoses, in *Protein Misfolding, Aggregation and Conformational Diseases* (Uversky, V. N., and Fink, A. L., Eds.) pp 239−276; Springer, New York.
(22) Dall'Acqua, S., Cervellati, R., Speroni, E., Costa, S., Guerra, M. C., Stella, L., Greco, E., and Innocenti, G. (2009) Phytochemical composition and antioxidant activity of *Laurus nobilis* L. leaf infusion. *J. Med. Food 12*, 869−876.
(23) Domon, B., and Costello, C. E. (1988) A systematic nomenclature for carbohydrate fragmentations in FAB-MS/MS spectra of glycoconjugates. *Glycoconjugate J. 5*, 397−409.
(24) Vallverdú-Queralt, A., Jáuregui, O., Medina-Remón, A., Andrés-Lacueva, C., and Lamuela-Raventós, R. M. (2010) Improved characterization of tomato polyphenols using liquid chromatography/electrospray ionization linear ion trap quadrupole Orbitrap mass spectrometry and liquid chromatography/electrospray ionization tandem mass spectrometry. *Rapid Commun. Mass Spectrom. 20*, 2986−2992.
(25) Cuyckens, F., and Claeys, M. (2004) Mass spectrometry in the structural analysis of flavonoids. *J. Mass Spectrom. 39*, 1−15.
(26) Ferreres, F., Silva, B. M., Andrade, P. B., Seabra, R. M., and Ferreira, M. A. (2003) Approach to the study of C-glycosyl flavones by ion trap HPLC-PAD-ESI/MS/MS: application to seeds of quince (*Cydonia oblonga*). *Phytochem. Anal. 14*, 352−359.
(27) Piccinelli, A. L., Mesa, M. G., Armenteros, D. M., Alfonso, M. A., Arevalo, A. C., Campone, L., and Rastrelli, L. (2008) HPLC PDA-MS and NMR characterization of *C*-glycosyl flavones in a hydroalcoholic extract of *Citrus aurantifolia* leaves with antiplatelet activity. *J. Agric. Food. Chem. 56*, 1574−1581.
(28) Negri, G., Santi, D., and Tabach, R. (2012) Chemical composition of hydroethanolic extracts from *Siparuna guianensis*, medicinal plant used as anxiolytics in Amazon region. *Rev. Bras. Farmacogn. 22*, 1024−1034.
(29) Sánchez-Rabaneda, F., Jáuregui, O., Casals, I., Andrés-Lacueva, C., Izquierdo-Pulido, M., and Lamuela-Raventós, R. M. (2003) Liquid chromatographic/electrospray ionization tandem mass spectrometric study of the phenolic composition of cocoa (*Theobroma cacao*). *J. Mass Spectrom. 38*, 35−42.
(30) Ferreres, F., Sousa, C., Valentao, P., Pereira, J. A., Seabra, R. M., and Andrade, P. B. (2007) *Tronchuda cabbage* flavonoids uptake by *Pieris brassicae*. *Phytochemistry 68*, 361−367.
(31) Cuyckens, F., Rozenberg, R., de Hoffmann, E., and Claeys, M. (2001) Structure characterization of flavonoid *O*-diglycosides by positive and negative nano-electrospray ionization ion trap mass spectrometry. *J. Mass Spectrom. 36*, 1203−1210.
(32) Ablajan, K., Abliz, Z., Shang, X. Y., He, J. M., Zhang, R. P., and Shi, J. G. (2006) Structural characterization of flavonol 3,7-di-*O*-glycosides and determination of the glycosylation position by using negative ion electrospray ionization tandem mass spectrometry. *J. Mass Spectrom. 41*, 353−360.
(33) Charrouf, Z., Hilali, M., Jauregui, O., Soufiaoui, M., and Guillaume, D. (2007) Separation and characterization of phenolic compounds in argan fruit pulp using liquid chromatography−negative electrospray ionization tandem mass spectroscopy. *Food Chem. 100*, 1398−1401.
(34) Flamini, R. (2013) Recent applications of mass spectrometry in the study of grape and wine polyphenols*ISRN Spectrosc.*, http://dx.doi.org/10.1155/2013/813563.
(35) Waridel, P., Wolfender, J. L., Ndjoko, K., Hobby, K. R., Major, H. J., and Hostettmann, K. (2001) Evaluation of quadrupole time-of-flight tandem mass spectrometry and ion-trap multiple-stage mass spectrometry for the differentiation of C-glycosidic flavonoid isomers. *J. Chromatogr., A. 926*, 29−41.
(36) Hvattum, E., and Ekeberg, D. (2003) Study of the collision-induced radical cleavage of flavonoid glycosides using negative electrospray ionization tandem quadrupole mass spectrometry. *J. Mass Spectrom. 38*, 43−49.
(37) Ayoub, N. A., Hashim, S. N., Hussein, S. A., Hegazi, N. M., Hassanein, H. M., and Nawwar, M. A. (2013) Hepatoprotective effect of bay leaves crude extract on primary cultured rat hepatocytes. *Eur. Sci. J. 3*, 647−655.
(38) Lee, S., Chung, S.-C., Lee, S.-H., Park, W., Oh, I., Mar, W., Shin, J., and Oh, K.-B. (2012) Acylated kaempferol glycosides from *Laurus nobilis* leaves and their inhibitory effects on Na^+/K^+-adenosine triphosphatase. *Biol. Pharm. Bull. 35*, 428−432.
(39) Prior, R. L., Huang, H., Gu, L., Wu, X., Bacchiocca, M., Howard, L., Hampsch-Woodill, M., Huang, D., Ou, B., and Jacob, R. (2003) Assays for hydrophilic and lipophilic antioxidant capacity (Oxygen Radical Absorbance Capacity (ORACFL)) of plasma and other biological and food samples. *J. Agric. Food Chem. 51*, 3273−3279.
(40) Vichai, V., and Kirtikara, K. (2006) Sulforhodamine B colorimetric assay for cytotoxicity screening. *Nat. Protoc. 3*, 1112−1116.
(41) Kleinkauf-Rocha, J., Bobermin, L. D., Machado Pde, M., Gonçalves, C. A., Gottfried, C., and Quincozes-Santos, A. (2013)

Lipoic acid increases glutamate uptake, glutamine synthetase activity and glutathione content in C6 astrocyte cell line. *Int. J. Dev. Neurosci. 31*, 165−170.

(42) Chan, F. K., Moriwaki, K., and De Rosa, M. J. (2013) Detection of necrosis by release of lactate dehydrogenase activity. *Methods Mol. Biol. 979*, 65−70.

(43) Barla, A., Topçua, G., Öksüza, S., Tümenb, G., and Kingston, D. G. I. (2007) Identification of cytotoxic sesquiterpenes from *Laurus nobilis* L. *Food Chem. 104*, 1478−1484.

(44) Shearman, M. S., Hawtin, S. R., and Tailor, V. J. (1995) The intracellular component of cellular 3-(4,5-dimethylthiazol-2-yl)-2,5-diphenyltetrazolium bromide (MTT) reduction is specifically inhibited by β-amyloid peptides. *J. Neurochem. 65*, 218−227.

(45) Liu, Y., and Schubert, D. (1997) Cytotoxic amyloid peptides inhibit cellular 3-(4,5-dimethylthiazol-2-yl)-2,5-diphenyltetrazolium bromide (MTT) reduction by enhancing MTT formazan exocytosis. *J. Neurochem. 69*, 2285−2293.

(46) Quintanilla, R. A., Muñoz, F. J., Metcalfe, M. J., Hitschfeld, M., Olivares, G., Godoy, J. A., and Inestrosa, N. C. (2005) Trolox and 17β-estradiol protect against amyloid β-peptide neurotoxicity by a mechanism that involves modulation of the Wnt signaling pathway. *J. Biol. Chem. 280*, 11615−11625.

(47) Vauzour, D., Vafeiadou, K., Rodriguez-Mateos, A., Rendeiro, C., and Spencer, J. P. (2008) The neuroprotective potential of flavonoids: a multiplicity of effects. *Genes Nutr. 3*, 115−126.

(48) Williams, R. J., and Spencer, J. P. (2011) Flavonoids, cognition, and dementia: actions, mechanisms, and potential therapeutic utility for Alzheimer disease. *Free Radical Biol. Med. 52*, 35−45.